



Pergamon

SCIENCE @ DIRECT[®]

Tetrahedron 59 (2003) 10419–10438

TETRAHEDRON

Tandem mass spectrometric analysis of rare earth(III) complexes: evaluation of the relative strength of their Lewis acidity

Hideyuki Tsuruta,^a Kentaro Yamaguchi^b and Tsuneo Imamoto^{a,*}

^aDepartment of Chemistry, Faculty of Science, Chiba University, Yayoi-cho, Inage-ku, Chiba 263-8522, Japan

^bChemical Analysis Center, Chiba University, Yayoi-cho, Inage-ku, Chiba 263-8522, Japan

Received 28 April 2003; accepted 11 June 2003

Abstract—Five series of rare earth(III) complexes coordinated with hexamethylphosphoramide, triethylphosphine oxide, trimethyl phosphate, *N,N'*-dimethylpropyleneurea, or dimethyl sulfoxide were subjected to tandem mass spectrometric analysis. The relative strength of the Lewis acidity of respective rare earth(III) species was evaluated using the peak intensity ratios of the product ions formed from the precursor ions (e.g. $[M(OTf)_2(hmpa)_2]^+$). The exceptionally strong Lewis acidity of scandium(III) and ytterbium(III) complexes was clearly indicated by this tandem MS analysis. The analysis also showed that the Lewis acidity of ytterbium(III) is stronger than that of lutetium(III) although the ionic radius of Yb^{3+} is larger than that of Lu^{3+} . The gadolinium break and the tetrad effect were observed in the Lewis acidity of the series of the lanthanide(III) complexes.

© 2003 Elsevier Ltd. All rights reserved.

1. Introduction

Trivalent rare earth compounds such as $CeCl_3$, $Yb(OTf)_3$, and $Sc(OTf)_3$ exhibit characteristic Lewis acid properties, and they activate oxygen and nitrogen functionalities to promote synthetically useful organic transformations.¹ For this reason, certain rare earth(III) compounds are frequently employed as highly efficient reagents or catalysts in modern organic synthesis. However, the origin of the characteristic chemical properties of rare earth(III) compounds is not yet well understood, although they are generally explained in terms of moderate to strong oxophilicity, long ionic radius, high coordination ability, and lanthanide contraction. The precise measurement of the relative strength of their Lewis acidity is necessary for the further development of new synthetic methods as well as for a comprehensive understanding of their intrinsic properties.

Tandem mass spectrometry is one of the most important methods in the structural analysis of materials.² It is especially useful in determining biologically important macromolecules such as peptides and proteins. For example, a mixture of peptides is analyzed by this tandem mass spectrometry without Edman degradation to elucidate each primary structure of the peptide components.³ In addition, the recent instrumental development of tandem

mass spectrometers, especially in combination with liquid chromatography, enables the easy structural analysis of sample mixtures.⁴

Tandem mass spectrometry is also used for physicochemical study on ionic species in gas phase.⁵ The method has been successfully employed to evaluate the relative proton affinity of bases and of the coordinative interaction between metal ions and ligands in gas phase. Furthermore, recent studies by Cooks et al. report that the kinetic method based on tandem mass spectrometry enables the chiral recognition and quantification of biologically important compounds such as amino acids, sugars, and α -hydroxy acids.⁶

On the other hand, we previously prepared a series of hexamethylphosphoramide (HMPA)-coordinated rare earth(III) trifluoromethanesulfonates (triflates), excluding the radioactive promethium complex, and determined their molecular structures by single crystal X-ray analysis.⁷ The revealed molecular structures are classified into the following three types: $[M(OTf)_2(hmpa)_4]OTf \cdot CHCl_3$ [$M=Y$, Ce, Pr, Nd, Sm, Eu, Gd, Tb, Dy, Ho, Er, Tm, Yb, Lu; $OTf=OSO_2CF_3$], $[Sc(OTf)_2(hmpa)_4]OTf$, and $[La(\eta^2-OTf)(OTf)(hmpa)_4]OTf \cdot CHCl_3$. An ORTEP drawing of the ytterbium complex, $[Yb(OTf)_2(hmpa)_4]OTf \cdot CHCl_3$, which belongs to the major structural type group, is shown in Figure 1 as a typical example. Four HMPA molecules are coordinated to the central metal ion to form an equatorial plane. Two triflate anions are located at the trans position,

Keywords: lanthanides; Lewis acidity; mass spectrometry.

* Corresponding author. Tel./fax: +81-43-290-2791;
e-mail: imamoto@faculty.chiba-u.jp

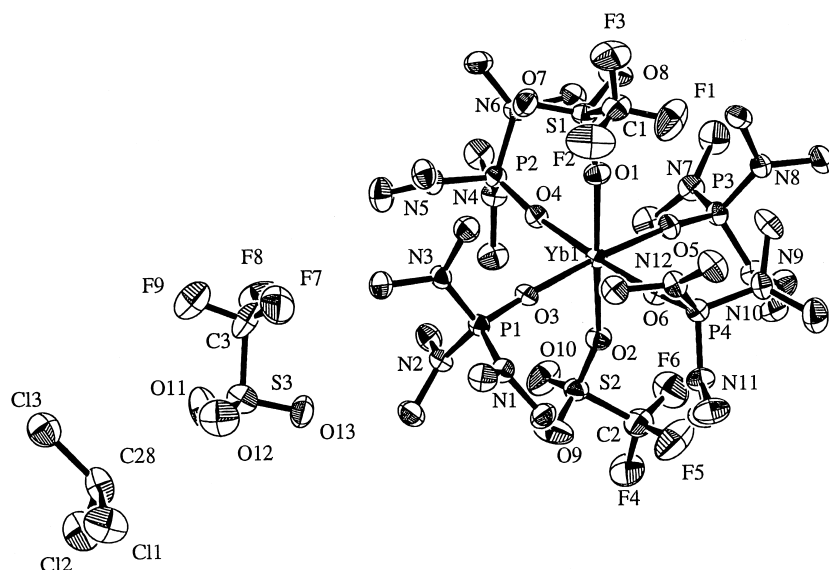


Figure 1. Crystal structure of $[Yb(OTf)_2(hmpa)_4]OTf \cdot CHCl_3$.

while a third triflate anion is not coordinated to the metal but interacts with chloroform through a hydrogen bond.

All the complexes, except the lanthanum complex, have almost the same hexa-coordinated octahedral structure. We expected that the similarity in molecular structure of the series of complexes is ideal for comparing physicochemical properties, and the HMPA complexes mentioned above are suitable substrates for tandem mass spectrometric analysis. Based on this idea, tandem mass spectrometric study was undertaken using HMPA-coordinated rare earth(III) inflates and other similar complexes bearing triethylphosphine oxide, trimethyl phosphate, dimethylpropyleneurea, or dimethyl sulfoxide as the ligand.⁸

2. Results and discussion

2.1. Structural analysis of HMPA-coordinated rare earth(III) triflates by tandem mass spectrometry

Our initial trial was directed to the normal FAB(+)MS measurement of a total of 16 HMPA-coordinated rare earth(III) triflates to obtain their fragmentation patterns. Figure 2 shows the MS spectrum of $[Er(OTf)_2(hmpa)_4]OTf$ as a representative example. The base peak, which was assigned as $[Er(OTf)_2(hmpa)_2]^+$, was observed at $m/z=824$. The molecular ion $[Er(OTf)_2(hmpa)_4]^+$ was detected as an appreciable peak, and the ion $[Er(OTf)_2(hmpa)_3]^+$ ($m/z=1003$), produced by the loss of one HMPA molecule

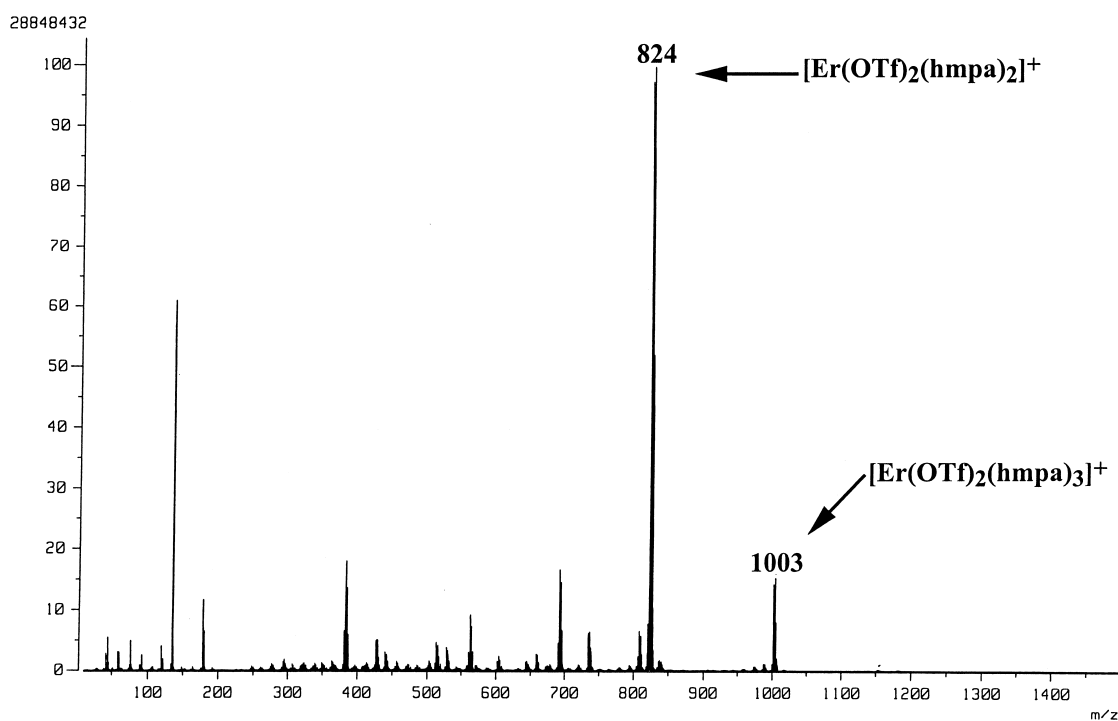


Figure 2. FAB(+)MS spectrum of $[Er(OTf)_2(hmpa)_4]OTf$.

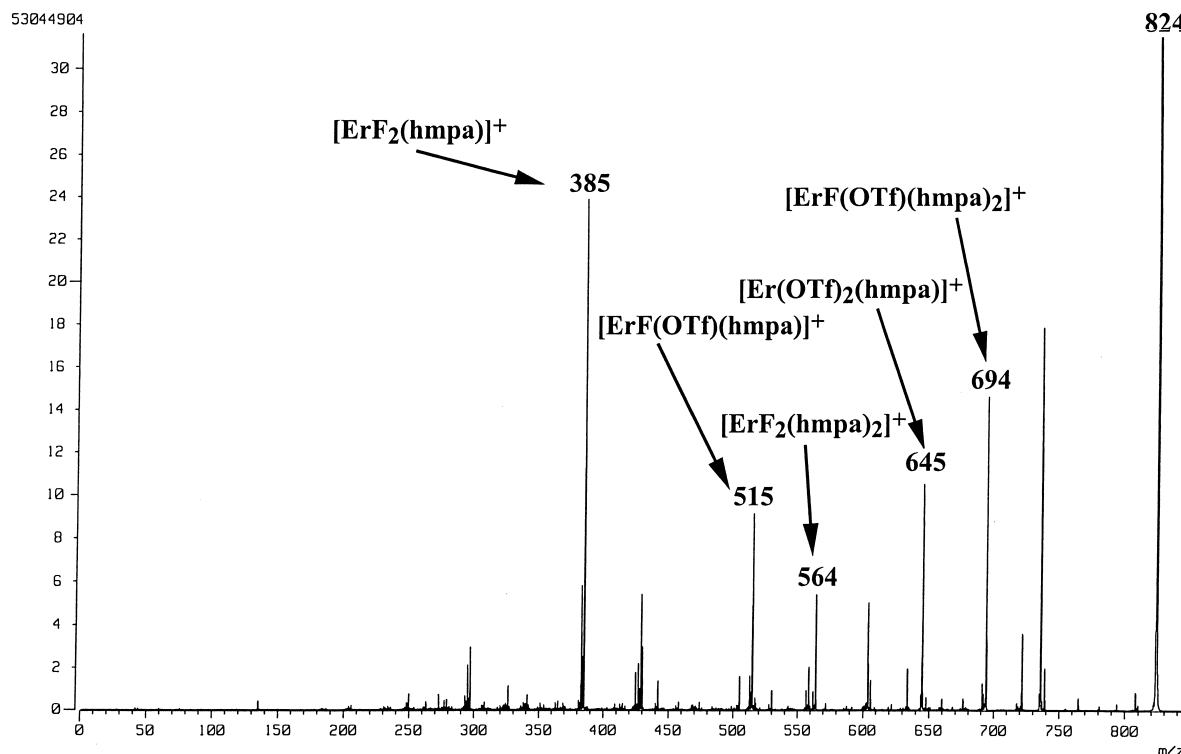


Figure 3. MS/MS spectrum of $[Er(OTf)_2(hmpa)_2]^+$ ($m/z=824$).

from the molecular ion, appeared as a strong peak.⁹ The distribution patterns of the fragmentation ions owing to erbium isotopes were consistent with those theoretically predicted.

The above results clearly indicate that the major fragmentation ions are produced by the loss of two HMPA molecules from the molecular ion. All other spectra of the series of the HMPA complexes have almost the same fragmentation patterns. It is particularly noteworthy that $[M(OTf)_2(hmpa)_2]^+$ was observed as the base peak without exception in these FAB(+) measurements. This base peak ion is tetra-coordinated with two triflate anions and two HMPA molecules to form a less sterically hindered complex. We considered that this steric environment around the metal center reflects precisely the electronic properties of rare earth(III) species in tandem MS spectrometric analysis, and hence $[M(OTf)_2(hmpa)_2]^+$ was selected as the precursor ion.

Tandem MS measurement was carried out using the collision-activated decomposition (CAD) method. The MS/MS spectrum of the precursor ion $[Er(OTf)_2(hmpa)_2]^+$ is shown in Figure 3 as an example, and the assigned major product ions are indicated in the spectrum. The conceivable fragmentation pathways from the precursor ion are illustrated in Figure 4. The deduction of mass number 179 is ascribed to the dissociation of HMPA (MW=179). The decrease in mass number 88 is due to the degradation of two dimethylamino groups from the HMPA ligand. On the other hand, Er–F bond formation occurs via the intramolecular rearrangement of the fluorine atom from carbon to erbium with the loss of (OTf–F) (mass number 130). The driving force of this rearrangement is the strong affinity of the fluoride ion with erbium(III). This observation is consistent

with the previously observed fact that thermal decomposition of lanthanum triflate leads to lanthanum fluoride.¹⁰

We carried out tandem mass spectroscopic analysis of all the other HMPA-coordinated rare earth(III) triflates using $[M(OTf)_2(hmpa)_2]^+$ as the precursor ion under exactly the same measurement conditions as those employed for the above-mentioned erbium complex. Each spectrum, which was obtained with very high reproducibility under the same ionization conditions, shows a similar fragmentation pattern involving $[MF(OTf)(hmpa)_2]^+$, $[M(OTf)_2(hmpa)]^+$, $[MF_2(hmpa)_2]^+$, $[MF(OTf)(hmpa)]^+$, and $[MF_2(hmpa)]^+$ as the major product ions,¹¹ while their relative intensities are different from each other, instead depending on each rare earth element. It is noteworthy that the spectrum of the europium complex is considerably different from the others. It shows not only the expected Eu(III) product ions ($[EuF(OTf)(hmpa)_2]^+$, $[Eu(OTf)_2(hmpa)]^+$, $[EuF_2(hmpa)_2]^+$, $[EuF(OTf)(hmpa)]^+$, and $[EuF_2(hmpa)]^+$) but also significantly strong europium(II) product ions (e.g. $[Eu(OTf)(hmpa)_2]^+$, $[Eu(OTf)(hmpa)]^+$, $[EuF(hmpa)]^+$) (Fig. 5). The formation of the latter Eu(II) product ions is responsible for the small oxidation–reduction potential between Eu(III) and Eu(II) (+0.35 V).¹² Similar fragmentations involving the reduction in the central metal atom were not observed in the samarium and ytterbium complexes although their oxidation–reduction potentials (Sm(II)/Sm(III): +1.55 V; Yb(II)/Yb(III): +1.05 V) are relatively small in comparison with those of other rare earth elements.¹²

We examined the relative intensities of the product ions in each spectrum and found that the intensity ratios largely differ depending on each element. Among them, the difference in the intensity ratios of $[MF(OTf)(hmpa)_2]^+$

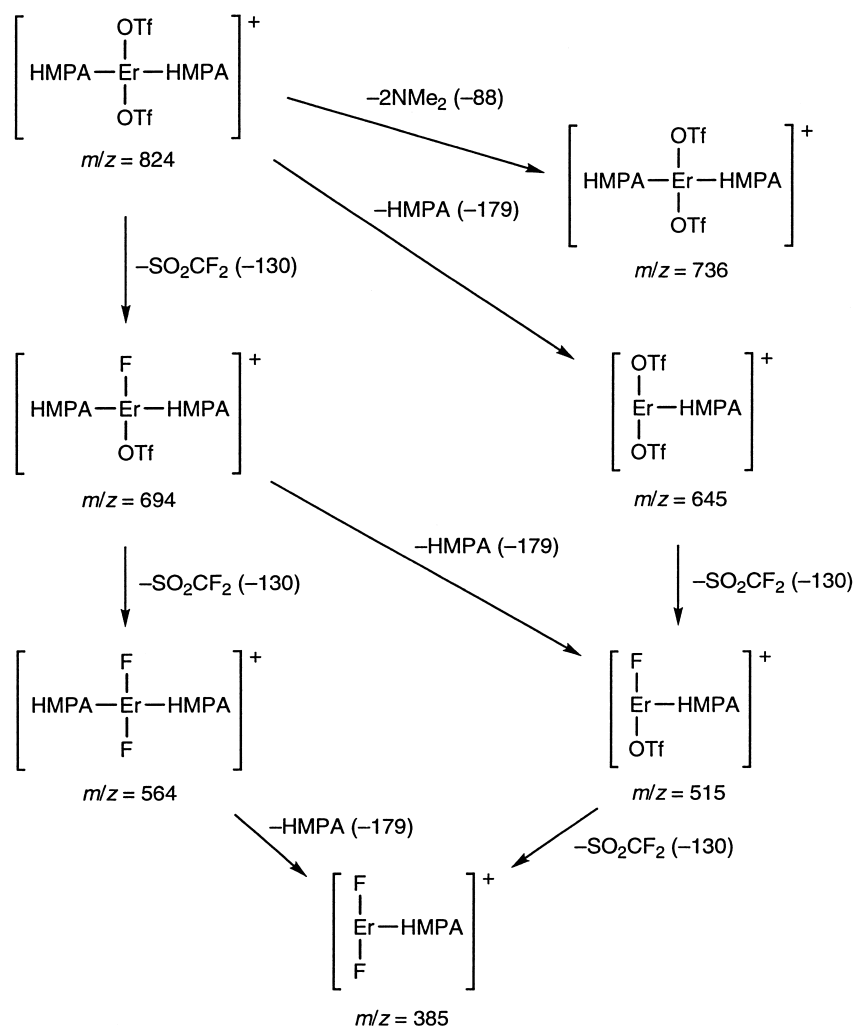


Figure 4. Cleavage pattern of $[Er(OTf)_2(hmpa)_2]^+$.

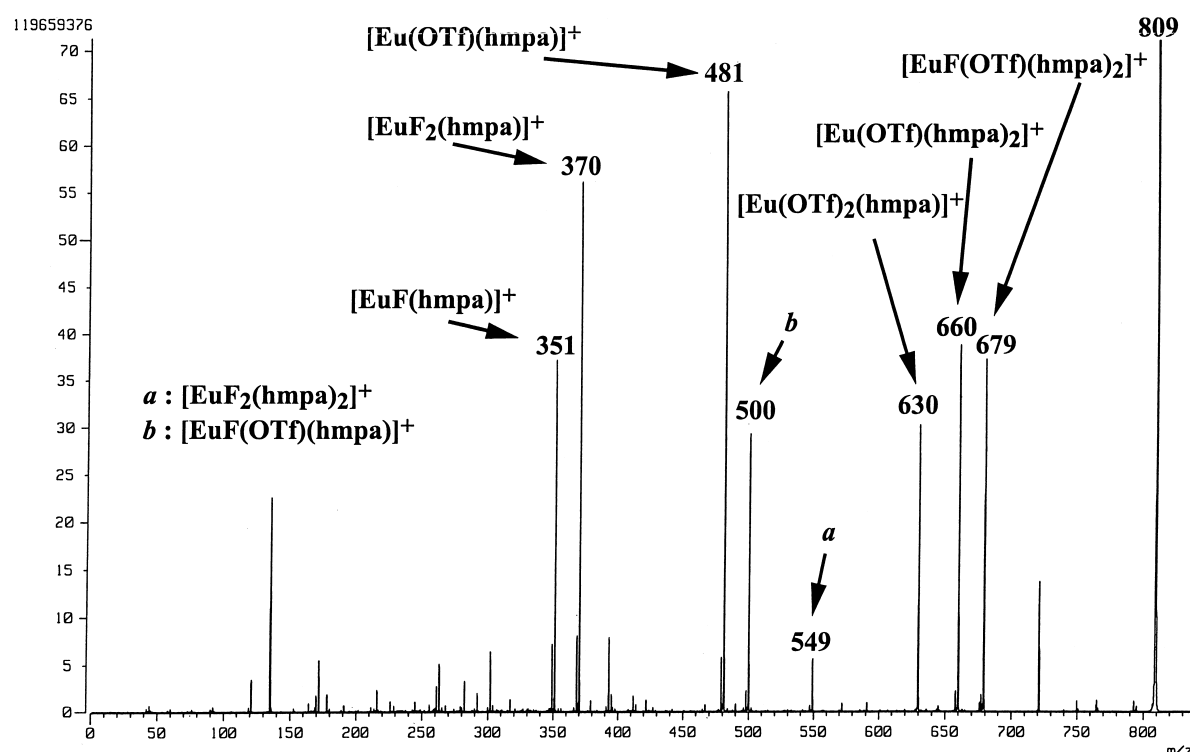


Figure 5. MS/MS spectrum of $[Eu(OTf)_2(hmpa)_2]^+$ ($m/z = 809$).

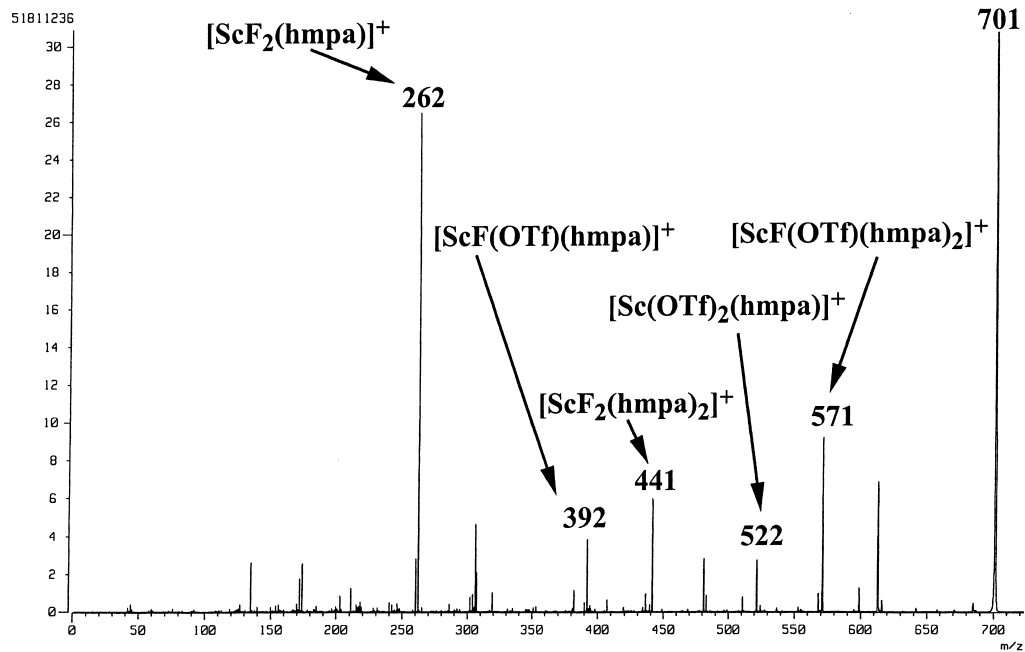


Figure 6. MS/MS spectrum of $[Sc(OTf)_2(hmpa)]^+$ ($m/z = 701$).

and $[M(OTf)_2(hmpa)]^+$ in each element is particularly significant. For example, a large value (3.5) and a small value (0.56) are observed for Sc and La, respectively, as shown in Figures 6 and 7. The ion $[MF(OTf)(hmpa)_2]^+$ is produced from the precursor ion by the M–OTf bond fission and the M–F bond formation. The formation of another ion, $[M(OTf)_2(hmpa)]^+$, is due to the loss of the neutral HMPA molecule from the precursor ion. Therefore, the intensity ratio reflects the ease of the M–OTf bond fission, the M–F bond formation, and the dissociation of the HMPA molecule from the central metal. It is postulated that the intensity ratio is proportional to the reaction rates of respective fragmenta-

tions because each fragmentation occurs independently and competitively (Scheme 1).¹³ In this hypothesis, the activation energy difference between respective fragmentations is represented by the logarithmic ratio of the ion intensities. In $\{[MF(OTf)(hmpa)_2]^+/[M(OTf)_2(hmpa)]^+\}$. Figure 8 shows the plots between the calculated quotients versus the atomic numbers. It is apparent that scandium has the largest quotient, followed by ytterbium, and lanthanum has the smallest. It is also clearly indicated that the quotients tend to increase with the increasing order of the atomic numbers. However, the value of ytterbium is somewhat larger than that of lutetium. A similar reversal is also

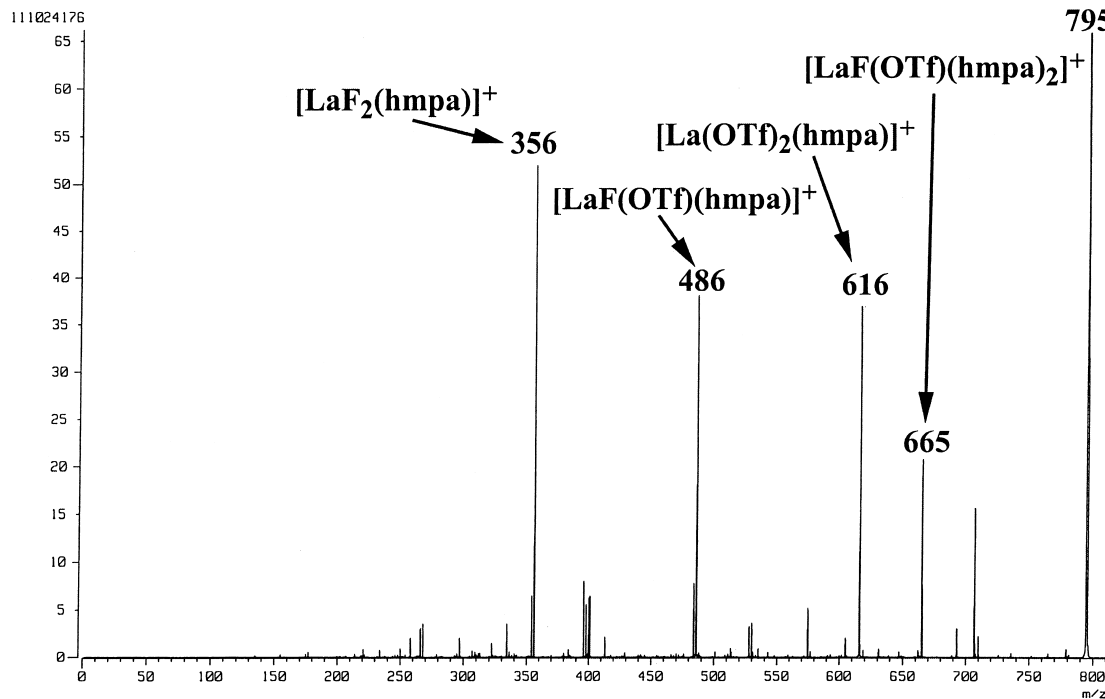
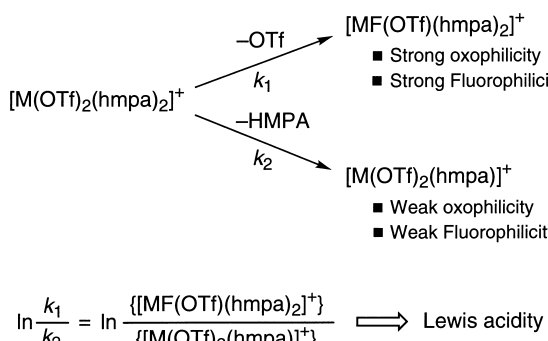
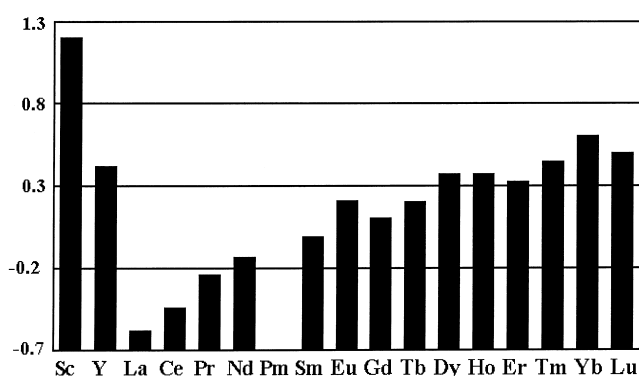


Figure 7. MS/MS spectrum of $[La(OTf)_2(hmpa)]^+$ ($m/z = 795$).



Scheme 1.

Figure 8. MS/MS ion peak ratio, $\ln\{[\text{MF(OTf)(hmpa)}_2]^+ / [\text{M(OTf)}_2(\text{hmpa})]^+\}$.

observed between europium and gadolinium, and holmium and erbium. The former reversal is regarded as the gadolinium break. These reversals indicate that the tetrad effect is manifested in this series of the MS/MS intensity ratio. It has been reported that the tetrad effect (inclined *W*-effect) represents the periodical change in the physical and chemical properties of the lanthanide(III) series for tetrads [(La, Ce, Pr, Nd), (Pm, Sm, Eu, Gd), (Gd, Tb, Dy, Ho), and (Er, Tm, Yb, Lu)].¹⁴ Some distinct tetrad effects have been already observed in the partition constants of lanthanide(III) salts in a liquid–liquid system,¹⁵ which are attributed to the ion stabilities that originate mainly from the quantum mechanical interelectronic repulsion energy of 4f electrons.^{14,16} The tetrad effect found in this study is also attributable to the same origin.

These phenomena can be rationalized by considering the major factors that produce respective product ions from the precursor ion. The conversion process from $[\text{M(OTf)}_2(\text{hmpa})_2]^+$ to $[\text{MF(OTf)(hmpa)}_2]^+$ involves the O–Tf bond fission with the simultaneous rearrangement of the fluorine atom to the central metal, and no HMPA molecules are dissociated in this step. Therefore, this process is affected by both oxophilicity and fluorophilicity. In other words, the element with strong oxophilicity and fluorophilicity promotes this process. On the other hand, conversion from $[\text{M(OTf)}_2(\text{hmpa})_2]^+$ to $[\text{M(OTf)}_2(\text{hmpa})]^+$ involves only the dissociation of one HMPA molecule, the two triflate ligands remaining attached to the central atom. The driving force of this process is responsible for the weak oxophilicity and weak fluorophilicity of each rare earth(III) species. Therefore, the quotient $\ln\{[\text{MF(OTf)(hmpa)}_2]^+ / [\text{M(OTf)}_2(\text{hmpa})]^+\}$

$(\text{hmpa})^+\}$ is a scale for the Lewis acidity (Scheme 1). These considerations clearly indicate that the Lewis acidities of scandium and ytterbium are the strongest among the rare earth elements. These results correspond to those obtained by single-crystal X-ray analysis of rare earth HMPA complexes.^{7,17} They are also consistent with the exceptionally high catalytic activity of scandium and ytterbium in Lewis acid-promoted organic transformations.¹⁸

The above results clearly indicate that the relative strength of the Lewis acidity of rare earths can be evaluated by the tandem mass spectrometric method. Unlike methods that use solutions or crystals, this measurement is carried out in very thin gaseous conditions with no appreciable interionic interaction, and hence the data are reflected from the properties of each precursor ion. Furthermore, the measurements of all the complexes of the series are carried out under exactly the same conditions. Hence, this method is ideal for the relative comparison of the physicochemical properties of rare earth elements. Another advantage of this method is that measurement can be conveniently carried out even though the sample materials are not always pure.

2.2. Structural analysis rare of earth(III) triflates bearing triethylphosphine oxides or trimethyl phosphate as the ligand

The above method was applied to analogous systems to examine generality. The complexes used are rare earth triflates bearing triethylphosphine oxide or trimethyl phosphate. Both ligands are sterically less hindered compared with HMPA, and therefore the steric repulsion between ligands might decrease in these complexes, and more precise electronic properties may be reflected in tandem mass spectrometric analysis.

At first, we tried to measure the spectra of triethylphosphine oxide (TEPO) complexes $[\text{M(OTf)}_2(\text{tepo})_4]^+\text{OTf}^-$. Before measuring the tandem MS we carried out FAB(+)MS for the complexes to select the precursor ion. A representative example of the spectra is shown in Figure 9 where the following three peaks were readily assigned: $[\text{Er(OTf)}_2(\text{tepo})_2]^+$ ($m/z=1002$; molecular ion peak), $[\text{Er(OTf)}_2(\text{tepo})_3]^+$ ($m/z=868$), $[\text{Er(OTf)}_2(\text{tepo})_2]^+$ ($m/z=734$; base ion peak). The fragmentation pattern is similar to the spectrum of the corresponding HMPA complex. Other triethylphosphine oxide complexes were also subjected to FAB(+)measurements to give almost the same fragmentation pattern. The base ion peak $[\text{M(OTf)}_2(\text{tepo})_2]^+$ was selected as the precursor ion for all the complexes of this series. The spectrum of the erbium complex is shown in Figure 10 as an example where $[\text{ErF(OTf)(tepo)}_2]^+$ ($m/z=604$), $[\text{Er(OTf)}_2(\text{tepo})]^+$ ($m/z=600$), $[\text{ErF}_2(\text{tepo})_2]^+$ ($m/z=474$), $[\text{ErF(OTf)(tepo)}]^+$ ($m/z=470$), and $[\text{ErF}_2(\text{tepo})]^+$ ($m/z=340$) appear as strong peaks. Similar fragmentation patterns were observed for the other complexes except the europium complex, whose spectrum involves fragmentation ions containing Eu(II) species, as similarly observed in the spectrum of the europium HMPA complex.

The values of $\ln\{[\text{MF(OTf)(tepo)}_2]^+ / [\text{M(OTf)}_2(\text{tepo})]^+\}$

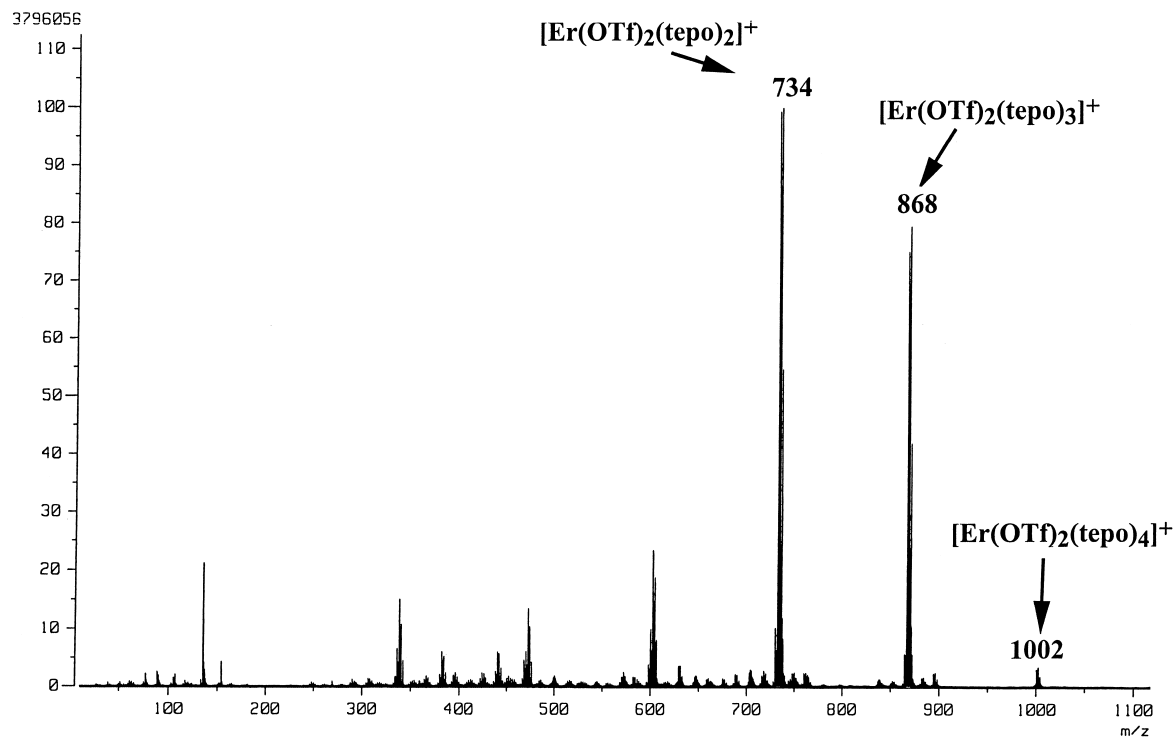


Figure 9. FAB(+)MS spectrum of $[\text{Er}(\text{OTf})_2(\text{tepo})_4]\text{OTf}$.

were calculated and were plotted versus atomic numbers. Figure 11 shows the results. It is apparent that, similar to the results of HMPA complexes, scandium gives the largest value and the gadolinium break is also observed.

A similar mass spectrometric analysis was also carried out

in the rare earth(III) triflates of trimethyl phosphate (TMP) complexes. The results are shown in Figure 12.

Tandem mass spectrometric analyses of three series of rare earth(III) triflate complexes having HMPA, TEPO, or TMP show almost the same results although the ligands are

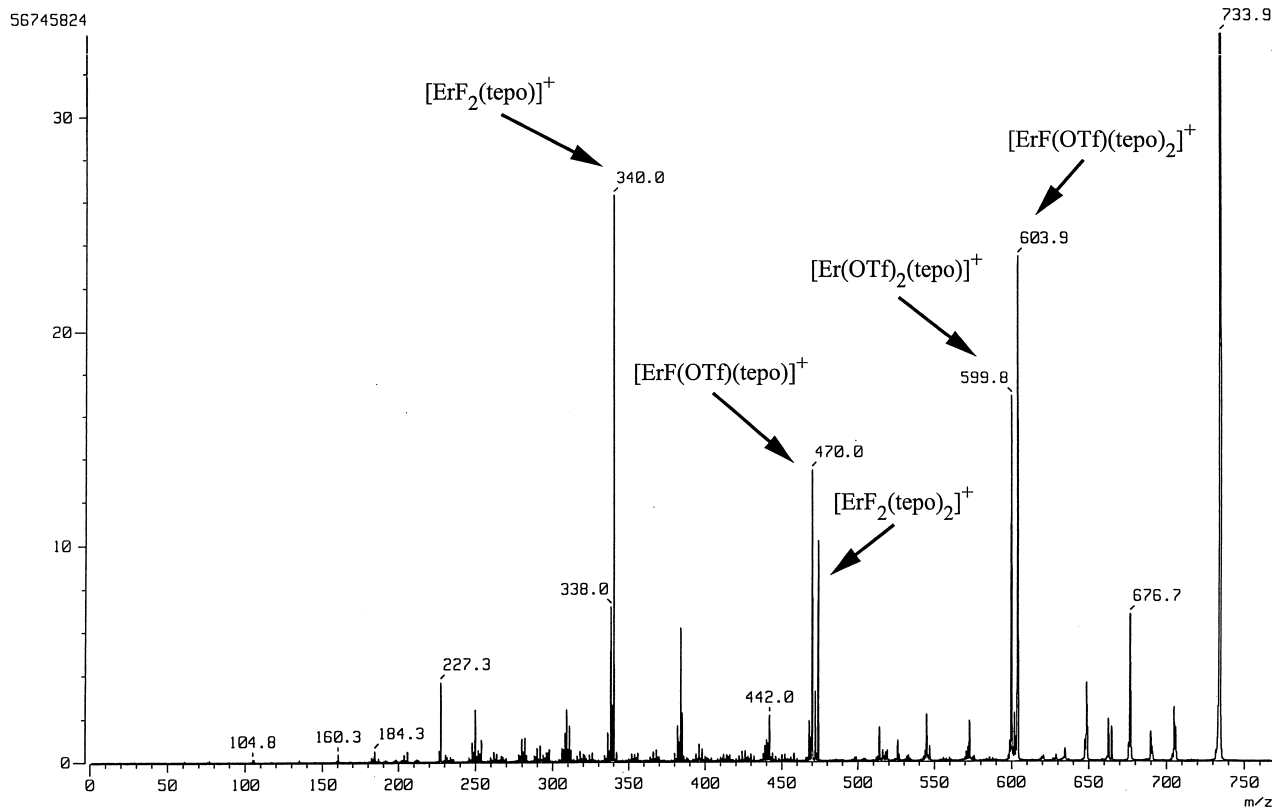


Figure 10. MS/MS spectrum of $[\text{Er}(\text{OTf})_2(\text{tepo})_2]^+$ ($m/z = 734$).

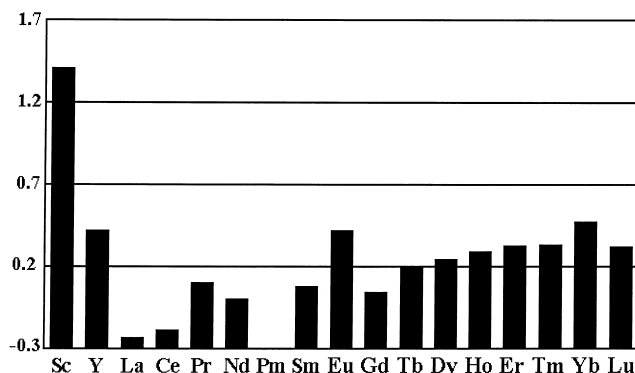


Figure 11. MS/MS ion peak ratio, $\ln\{[\text{MF}(\text{OTf})(\text{tepo})_2]^+ / [\text{M}(\text{OTf})_2-\text{tepo}]^+\}$.

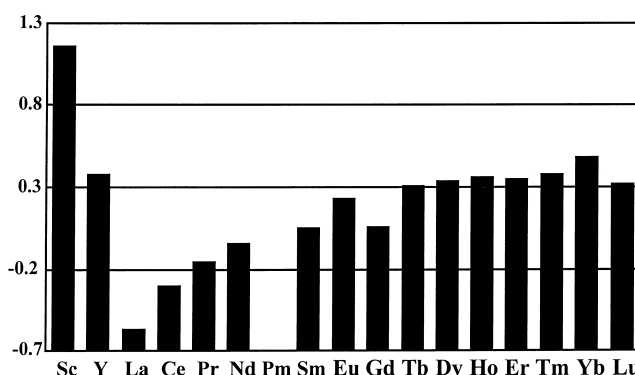


Figure 12. MS/MS ion peak ratio, $\ln\{[\text{MF}(\text{OTf})(\text{tmp})_2]^+ / [\text{M}(\text{OTf})_2-(\text{tmp})]^+\}$.

different in steric size and electron density at the donor oxygen atom. Therefore, it can be concluded that neither the steric nor the electronic effects of the coordinating ligands affect the results.

2.3. Structural analysis of rare earth(III) triflates bearing *N,N'*-dimethylpropyleneurea or dimethyl sulfoxide as the ligand

Most of the organic transformations promoted by rare earth(III) catalysts or reagents involve carbonyl compounds substrates. The reactions proceed through the initial activation of the carbonyl functional groups through coordinative interaction with rare earth(III) species. We expected that the tandem mass spectrometric analysis of a series of rare earth(III) complexes with carbonyl compounds would provide information reflecting their Lewis acid properties in real reaction systems. Using of electrospray mass spectrometric analysis, we previously demonstrated the formation of complexes of cerium(III) chloride and 2-cyclopentenone in methanol.¹⁹ Based on this, we attempted to isolate the rare earth complexes of simple ketones such as acetone and cyclopentanone, but we failed because they were extremely labile. Use of a ligand with greater electron-donating properties, *N,N'*-dimethylpropyleneurea (DMPU) (tetrahydro-2-pyrimidinone), led to the successful isolation of the corresponding rare earth(III) triflate complexes.²⁰ The DMPU complexes isolated were subjected to mass spectrometric analysis under almost the same conditions as for the previously mentioned HMPA

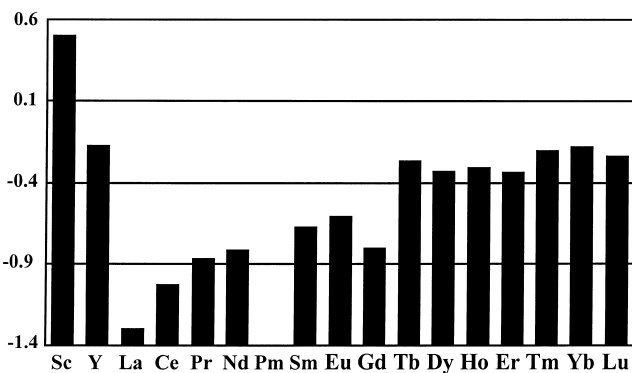


Figure 13. MS/MS ion peak ratio, $\ln\{[\text{MF}(\text{OTf})(\text{dmpu})_2]^+ / [\text{M}(\text{OTf})_2-(\text{dmpu})]^+\}$.

complexes. The FAB(+) measurements of the DMPU complexes indicate that $[\text{M}(\text{OTf})_2(\text{dmpu})_3]^+$ and $[\text{M}(\text{OTf})_2(\text{dmpu})_2]^+$ were the major fragment ions. The latter ion $[\text{M}(\text{OTf})_2(\text{dmpu})_2]^+$, which was observed as the base ion peak, was selected as the precursor ion in this series of complexes. The MS/MS ion peak ratios $\ln\{[\text{MF}(\text{OTf})(\text{dmpu})_2]^+ / [\text{M}(\text{OTf})_2(\text{dmpu})]^+\}$ versus atomic number is shown in Figure 13.

The figure shows that scandium has the largest quotient, ytterbium has the second, and lanthanum has the smallest. The gadolinium break and the tetrad effect are also observed in this system. The results suggest that the degree of carbonyl activation in real reaction systems is proportional to the quotient of each rare earth element.

The generality of the tandem mass spectrometric method was also tested using dimethyl sulfoxide complexes. Figure 14 shows the MS/MS ion peak ratio $\ln\{[\text{MF}(\text{OTf})(\text{dmso})_2]^+ / [\text{M}(\text{OTf})_2(\text{dmso})]^+\}$ versus atomic number, which clearly justifies this methodology.

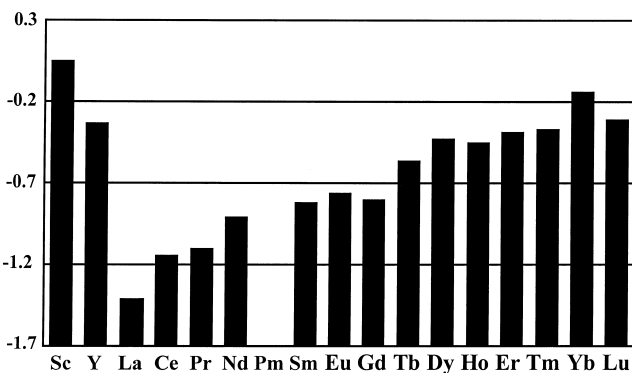


Figure 14. MS/MS ion peak ratio, $\ln\{[\text{MF}(\text{OTf})(\text{dmso})_2]^+ / [\text{M}(\text{OTf})_2-(\text{dmso})]^+\}$.

Tandem mass spectrometric analysis of five series of rare earth complexes provided almost the same results, indicating the strong Lewis acidity of scandium and ytterbium and the existence of the gadolinium break and the tetrad effect. Previously reported methods that use solutions or crystalline solids cannot be conducted under exactly the same conditions because of the change of coordination number and the inevitable intermolecular interactions. In contrast,

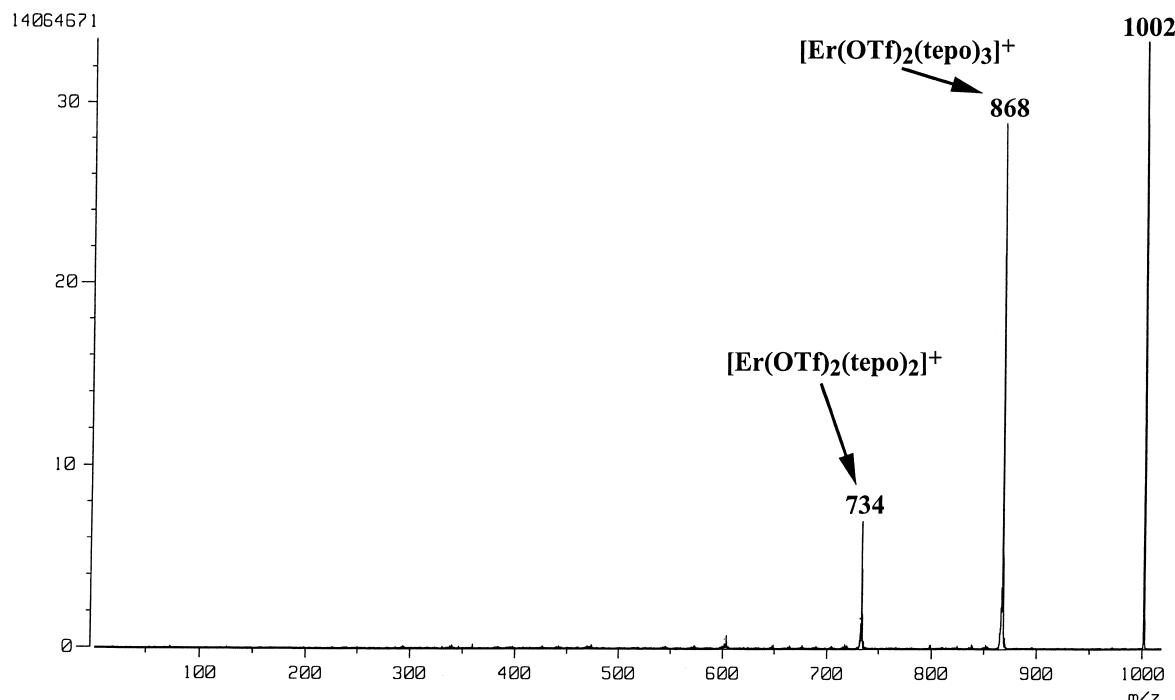


Figure 15. MS/MS spectrum of $[Er(OTf)_2(tepo)_4]^+$.

the method using tandem mass spectrometry is very useful for the relative evaluation of physicochemical properties.

2.4. Evaluation of the relative strength of the oxophilicity of rare earth(III) complexes

Previous sections show the evaluation of the relative Lewis acidity by tandem mass spectroscopy. However, Lewis acidity involves not only oxophilicity but also fluorophilicity, since one of the selected product ions is formed via the intramolecular rearrangement of the fluorine atom. It is important to evaluate oxophilicity only because the activation of oxygen functionalities plays an important role in Lewis acid-promoted organic reactions. We considered that oxophilicity alone could be evaluated by selecting product ions that are produced via the loss of a neutral oxygen donor ligand alone. After careful examination of our mass spectrometric data, we found that $[M(OTf)_2(tepo)_4]^+$ is the most suitable precursor ion although the ion intensity is not strong. The MS/MS spectrum of $[Er(OTf)_2(tepo)_4]^+$ is shown in Figure 15 as a

representative example, where two strong ions, $[Er(OTf)_2(tepo)_3]^+$ and $[Er(OTf)_2(tepo)_2]^+$, clearly appear as the product ions. The logarithmic quotients of $\ln\{[M(OTf)_2(tepo)_3]^+/[M(OTf)_2(tepo)_2]^+\}$ of all TEPO-coordinated rare earth(III) triflates were obtained based on their intensity ratios. The plots of the values versus atomic number are illustrated in Figure 16. Surprisingly, a graphical pattern analogous to that shown in previous sections was produced, indicating exceptionally large quotients of scandium and ytterbium. It is also noteworthy that the gadolinium break and the tetrad effect are clearly manifested in this case.

To examine the generality of the method, we then measured a series of TEPO-coordinated rare earth(III) chlorides. The analysis was carried out in a similar manner as for the above triflate complexes. However, the tandem MS of $[EuCl_2(tepo)_3]^+$ afforded divalent europium ions $[EuCl(tepo)]^+$ and $[EuCl(tepo)]^+$ as the strong peaks. For this reason, we excluded the unreliable value of the europium spectrum for analysis. Figure 17 shows the analysis results based on the ion peak ratios of $[MCl_2(tepo)]^+/[MCl_2(tepo)_2]^+$. It also

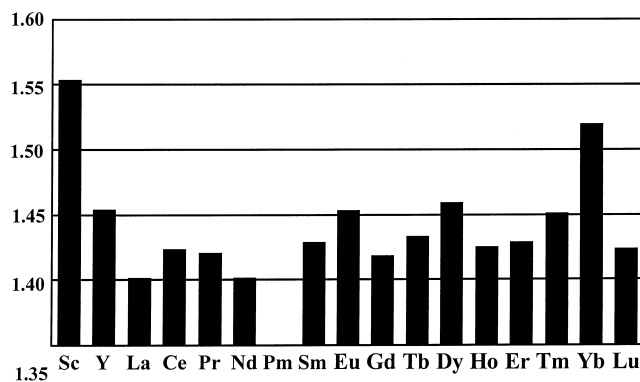


Figure 16. MS/MS ion peak ratio, $\ln\{[M(OTf)_2(tepo)_3]^+/[M(OTf)_2(tepo)_2]^+\}$.

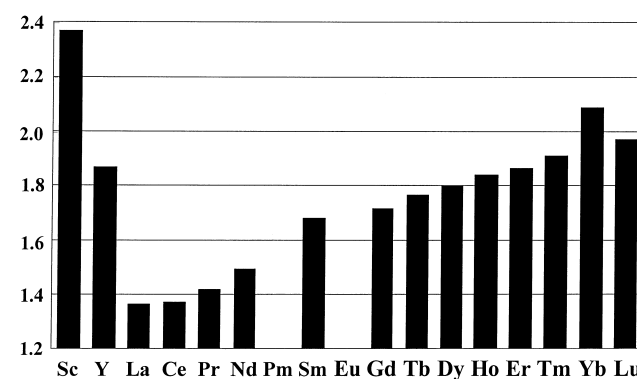


Figure 17. MS/MS ion peak ratio, $\ln\{[MCl_2(tepo)]^+/[MCl_2(tepo)_2]^+\}$.

shows large quotients of scandium and ytterbium, while the gadolinium break and the tetrad effect are not clearly observed.

All the data obtained in this investigation using five series of rare earth(III) complexes clearly demonstrate that scandium has the highest Lewis acidity followed by ytterbium.²¹ This is consistent with the exceptionally high catalytic activity of both Sc(III) and Yb(III) compounds in a number of Lewis acid-promoted reactions. The high Lewis acidity of scandium(III) and ytterbium(III) is mainly ascribed to their small ionic radii. The higher acidity of Yb(III) relative to Lu(III) may originate from an incomplete number of electrons (13) in the seven 4f orbitals. The insufficiently filled state, which has a tendency to become a filled state (f¹⁴), renders the Yb(III) ion more electron-attractive than the Lu(III) ion.

3. Conclusion

Five series of rare earth(III) complexes coordinated with oxygen donor ligands have been analyzed by tandem mass spectrometry. The relative strength of the Lewis acidity of the complexes was evaluated by the peak intensity ratios of the product ions. The exceptionally strong Lewis acidity of the scandium(III) and ytterbium(III) complexes was clearly indicated by this method together with the gadolinium break and the tetrad effect. This is the first application of tandem mass spectrometry in the study on structure–reactivity relationships of rare earth compounds.

4. Experimental

4.1. Preparation of hexamethylphosphoramide-coordinated rare earth(III) triflates. General procedure

Anhydrous rare earth(III) triflate (5 mmol) was stirred in dry THF (30 mL) containing HMPA (4.4 mL, 25 mmol) in an argon atmosphere for 1 h. The solvent was evaporated and the residual solid was washed with ethyl acetate to produce a powder. Pure complexes were obtained by recrystallization from chloroform/ethyl acetate (1:2–1:4). The structures of all the complexes obtained were confirmed by single-crystal X-ray analyses.⁷

4.2. Preparation of triethylphosphine oxide-coordinated rare earth(III) triflates. General procedure

Anhydrous rare earth(III) triflate (1 mmol) was stirred in dry THF (6 mL) containing triethylphosphine oxide (670 mg, 5 mmol) in an argon atmosphere for 1 h. The solvent was evaporated and the residual solid was washed with ethyl acetate. The product was used for mass spectroscopic analysis without further purification.

4.3. Preparation of trimethyl phosphate-coordinated rare earth(III) triflates. General procedure

Anhydrous rare earth(III) triflate (1 mmol) was stirred in dry THF (6 mL) containing trimethyl phosphate (700 mg, 5 mmol) in an argon atmosphere for 1 h. The solvent was

evaporated and the residual solid was washed with ethyl acetate. The product was used for mass spectroscopic analysis without further purification.

4.4. Preparation of N,N'-dimethylpropyleneurea rare earth(III) triflates. A typical procedure²⁰

A hot methanol solution (100 mL) of N,N'-dimethylpropyleneurea (tetrahydro-2-pyrimidinone) (4.0 g, 40 mmol) was added to a solution of anhydrous samarium(III) triflate (3.0 g, 5 mmol) in MeOH (30 mL) at room temperature. After 1 h, the solvent was removed under reduced pressure to give [Sm(dmpu)₈](OTf)₃ as a white powder (6.2 g, 88%). Mp 206–208°C.

4.5. Preparation of dimethyl sulfoxide-coordinated rare earth(III) triflates. General procedure

Anhydrous rare earth(III) triflate (1 mmol) was stirred in dry THF (6 mL) containing dimethyl sulfoxide (391 mg, 5 mmol) in an argon atmosphere for 1 h. The solvent was evaporated and the residual solid was washed with ethyl acetate. The product was used for mass spectroscopic analysis without further purification.

4.6. Preparation of triethylphosphine oxide-coordinated rare earth(III) chlorides. General procedure

Anhydrous rare earth(III) chloride (1 mmol) was stirred in dry THF (6 mL) containing triethylphosphine oxide (670 mg, 5 mmol) in an argon atmosphere for 1 h. The solvent was evaporated and the residual solid was washed with ethyl acetate. The product was used for mass spectroscopic analysis without further purification.

4.7. Mass spectrometric measurements

All mass spectra were obtained on JEOL JMS-700T (BE/BE Tandem MS). m-Nitrobenzyl alcohol was chosen as the FAB matrix.

The following MS/MS measurement conditions were applied to $[M(OTf)_2(hmpa)_2]^+$, $[M(OTf)_2(tepo)_2]^+$, $[M(OTf)_2(tmp)_2]^+$, $[M(OTf)_2(dmpu)_2]^+$, $[M(OTf)_2(dmso)_2]^+$, $[M(OTf)_2(tepo)_2]^+$, and $[MCl_2(tepo)_2]^+$.

Ion source	FAB(+)	Acceleration voltage	10 kV
MSI resolution	2000	MS2 resolution	1000
Collision gas	Xe	Collision cell voltage	0.5–3 kV
Transmission	ca. 20%	Data type	Profile-spectra
Scan range	0–900	All range scan speed	20 s
Repetition time	15 s	Times	10

4.8. Spectral data

4.8.1. FAB(+)MS spectra of tetrakis(hexamethylphosphoramide) rare earth(III) triflates. $[Sc(OTf)_2(hmpa)_4]OTf$. m/z 701 (100%), 880 (34%).

$[Y(OTf)_2(hmpa)_4]OTf$. m/z 745 (100%), 924 (46%), 1103 (2%).

$[La(OTf)_2(hmpa)_4]OTf$. m/z 795 (100%), 974 (34%).

[Ce(OTf)₂(hmpa)₄]OTf. *m/z* 796 (100%), 975 (41%), 1154 (1%).

[Pr(OTf)₂(hmpa)₄]OTf. *m/z* 797 (100%), 976 (34%).

[Nd(OTf)₂(hmpa)₄]OTf. *m/z* 798 (¹⁴²Nd, 93%), 799 (¹⁴³Nd, 61%), 800 (¹⁴⁴Nd, 100%), 801 (¹⁴⁵Nd, 52%), 802 (¹⁴⁶Nd, 74%), 977 (¹⁴²Nd, 38%), 978 (¹⁴³Nd, 29%), 979 (¹⁴⁴Nd, 44%), 980 (¹⁴⁵Nd, 25%), 981 (¹⁴⁶Nd, 32%), 1156 (¹⁴²Nd, 1%), 1158 (¹⁴⁴Nd, 1%) 1160 (¹⁴⁶Nd, 1%).

[Sm(OTf)₂(hmpa)₄]OTf. *m/z* 803 (¹⁴⁷Sm, 55%), 804 (¹⁴⁸Sm, 52%), 805 (¹⁴⁹Sm, 63%), 806 (¹⁵⁰Sm, 44%), 808 (¹⁵²Sm, 100%), 810 (¹⁵⁴Sm, 91%), 982 (¹⁴⁷Sm, 20%), 983 (¹⁴⁸Sm, 21%), 984 (¹⁴⁹Sm, 25%), 985 (¹⁵⁰Sm, 17%), 987 (¹⁵²Sm, 37%), 989 (¹⁵⁴Sm, 34%), 1166 (¹⁵²Sm, 1%), 1158 (¹⁵⁴Sm, 1%).

[Eu(OTf)₂(hmpa)₄]OTf. *m/z* 807 (¹⁵¹Eu, 84%), 809 (¹⁵³Eu, 100%), 986 (¹⁵¹Eu, 30%), 988 (¹⁵³Eu, 36%).

[Gd(OTf)₂(hmpa)₄]OTf. *m/z* 810 (¹⁵⁴Gd, 10%), 811 (¹⁵⁵Gd, 51%), 812 (¹⁵⁶Gd, 79%), 813 (¹⁵⁷Gd, 71%), 814 (¹⁵⁸Gd, 100%), 816 (¹⁶⁰Gd, 81%), 990 (¹⁵⁵Gd, 13%), 991 (¹⁵⁶Gd, 20%), 992 (¹⁵⁷Gd, 19%), 993 (¹⁵⁸Gd, 26%), 995 (¹⁶⁰Gd, 20%).

[Tb(OTf)₂(hmpa)₄]OTf. *m/z* 815 (100%), 994 (31%), 1173 (1%).

[Dy(OTf)₂(hmpa)₄]OTf. *m/z* 816 (¹⁶⁰Dy, 10%), 817 (¹⁶¹Dy, 57%), 818 (¹⁶²Dy, 85%), 819 (¹⁶³Dy, 90%), 820 (¹⁶⁴Dy, 100%), 995 (¹⁶⁵Dy, 3%), 996 (¹⁶⁶Dy, 19%), 997 (¹⁶²Dy, 30%), 998 (¹⁶³Dy, 33%), 999 (¹⁶⁴Dy, 36%), 1076 (¹⁶²Dy, 1%), 1077 (¹⁶³Dy, 1%), 1078 (¹⁶⁴Dy, 1%).

[Ho(OTf)₂(hmpa)₄]OTf. *m/z* 821 (100%), 1000 (41%), 1179 (1%).

[Er(OTf)₂(hmpa)₄]OTf. *m/z* 820 (¹⁶⁴Er, 8%), 822 (¹⁶⁶Er, 98%), 823 (¹⁶⁷Er, 84%), 825 (¹⁶⁸Er, 100%), 827 (¹⁷⁰Er, 2%), 1001 (¹⁶⁶Er, 14%), 1002 (¹⁶⁷Er, 13%), 1003 (¹⁶⁸Er, 15%), 1005 (¹⁷⁰Er, 8%).

[Tm(OTf)₂(hmpa)₄]OTf. *m/z* 825 (100%), 1004 (29%), 1183 (1%).

[Yb(OTf)₂(hmpa)₄]OTf. *m/z* 826 (¹⁷⁰Yb, 10%), 827 (¹⁷¹Yb, 41%), 828 (¹⁷²Yb, 68%), 829 (¹⁷³Yb, 59%), 830 (¹⁷⁴Yb, 100%), 832 (¹⁷⁶Yb, 45%), 1006 (¹⁷¹Yb, 12%), 1007 (¹⁷²Yb, 20%), 1008 (¹⁷³Yb, 18%), 1009 (¹⁷⁴Yb, 28%), 1011 (¹⁷⁶Yb, 13%).

[Lu(OTf)₂(hmpa)₄]OTf. *m/z* 831 (100%), 1010 (29%), 1189 (1%).

4.8.2. FAB(–)MS spectra of tetrakis(hexamethylphosphoramide) rare earth(III) triflates. [Sc(OTf)₂(hmpa)₄]OTf. *m/z* 641 (55%), 820 (29%), 999 (22%), 1178 (2%), 1357 (2%).

[Y(OTf)₂(hmpa)₄]OTf. *m/z* 685 (51%), 864 (16%), 1043 (12%), 1401 (5%).

[La(OTf)₂(hmpa)₄]OTf. *m/z* 735 (46%), 914 (5%), 1092 (1%).

[Er(OTf)₂(hmpa)₄]OTf. *m/z* 762 (¹⁶⁶Er, 1%), 763 (¹⁶⁷Er, 1%), 764 (¹⁶⁸Er, 2%), 766 (¹⁷⁰Er, 2%), 943 (¹⁶⁸Er, 1%).

[Yb(OTf)₂(hmpa)₄]OTf. *m/z* 767 (¹⁷¹Yb, 7%), 768 (¹⁷²Yb, 11%), 769 (¹⁷³Yb, 10%), 770 (¹⁷⁴Yb, 19%), 772 (¹⁷⁶Yb, 3%), 946 (¹⁷¹Yb, 3%), 947 (¹⁷²Yb, 4%), 948 (¹⁷³Yb, 4%), 949 (¹⁷⁴Yb, 6%), 951 (¹⁷⁶Yb, 4%), 1125 (¹⁷¹Yb, 2%), 1126 (¹⁷²Yb, 3%), 1127 (¹⁷³Yb, 3%), 1128 (¹⁷⁴Yb, 4%), 1130 (¹⁷⁶Yb, 3%), 1483 (¹⁷¹Yb, 1%), 1484 (¹⁷²Yb, 1%), 1485 (¹⁷³Yb, 1%), 1486 (¹⁷⁴Yb, 1%), 1488 (¹⁷⁶Yb, 1%).

4.8.3. MS/MS spectra of precursor ions [M(OTf)₂(hmpa)₂]⁺. [Sc(OTf)₂(hmpa)₂]⁺. Precursor ion: *m/z* 701. Product ions: *m/z* 262 ([ScF₂(hmpa)]⁺, 26.55%), 392 ([ScF(OTf)(hmpa)]⁺, 3.84%), 441 ([ScF₂(hmpa)₂]⁺, 5.98%), 522 ([Sc(OTf)₂(hmpa)]⁺, 2.76%), 571 ([ScF(OTf)(hmpa)₂]⁺, 9.24%).

[Y(OTf)₂(hmpa)₂]⁺. Precursor ion: *m/z* 745. Product ions: *m/z* 306 ([YF₂(hmpa)]⁺, 43.64%), 436 ([YF(OTf)(hmpa)]⁺, 21.43%), 485 ([YF₂(hmpa)₂]⁺, 10.69%), 566 ([Y(OTf)₂(hmpa)]⁺, 23.19%), 615 ([YF(OTf)(hmpa)₂]⁺, 35.34%).

[La(OTf)₂(hmpa)₂]⁺. Precursor ion: *m/z* 745. Product ions: *m/z* 356 ([LaF₂(hmpa)]⁺, 52.12%), 486 ([LaF(OTf)(hmpa)]⁺, 38.28%), 535 ([LaF₂(hmpa)₂]⁺, 0.91%), 615 ([La(OTf)₂(hmpa)]⁺, 37.06%), 665 ([LaF(OTf)(hmpa)₂]⁺, 20.82%).

[Ce(OTf)₂(hmpa)₂]⁺. Precursor ion: *m/z* 796. Product ions: *m/z* 357 ([CeF₂(hmpa)]⁺, 74.76%), 487 ([CeF(OTf)(hmpa)]⁺, 42.49%), 536 ([CeF₂(hmpa)₂]⁺, 1.37%), 617 ([Ce(OTf)₂(hmpa)]⁺, 41.06%), 666 ([CeF(OTf)(hmpa)₂]⁺, 26.55%).

[Pr(OTf)₂(hmpa)₂]⁺. Precursor ion: *m/z* 797. Product ions: *m/z* 358 ([PrF₂(hmpa)]⁺, 34.94%), 488 ([PrF(OTf)(hmpa)]⁺, 21.50%), 537 ([PrF₂(hmpa)₂]⁺, 0.93%), 618 ([Pr(OTf)₂(hmpa)]⁺, 18.44%), 667 ([PrF(OTf)(hmpa)₂]⁺, 14.61%).

[Nd(OTf)₂(hmpa)₂]⁺. Precursor ion: *m/z* 800. Product ions: *m/z* 361 ([NdF₂(hmpa)]⁺, 33.72%), 491 ([NdF(OTf)(hmpa)]⁺, 21.60%), 540 ([NdF₂(hmpa)₂]⁺, 1.72%), 621 ([Nd(OTf)₂(hmpa)]⁺, 19.88%), 670 ([NdF(OTf)(hmpa)₂]⁺, 17.37%).

[Sm(OTf)₂(hmpa)₂]⁺. Precursor ion: *m/z* 808. Product ions: *m/z* 369 ([SmF₂(hmpa)]⁺, 45.63%), 499 ([SmF(OTf)(hmpa)]⁺, 19.35%), 548 ([SmF₂(hmpa)₂]⁺, 2.71%), 629 ([Sm(OTf)₂(hmpa)]⁺, 19.11%), 678 ([SmF(OTf)(hmpa)₂]⁺, 19.02%).

[Eu(OTf)₂(hmpa)₂]⁺. Precursor ion: *m/z* 809. Product ions: *m/z* 351 ([EuF₂(hmpa)]⁺, 37.27%), 370 ([EuF₂(hmpa)]⁺, 56.25%), 481 ([EuF(hmpa)]⁺, 65.97%), 500 ([EuF(OTf)(hmpa)]⁺, 29.35%), 549 ([EuF₂(hmpa)₂]⁺, 5.59%), 630 ([Eu(OTf)₂(hmpa)]⁺, 30.31%), 660 ([Eu(OTf)(hmpa)₂]⁺, 38.93%), 679 ([EuF(OTf)(hmpa)₂]⁺, 37.41%).

$[Gd(OTf)_2(hmpa)_2]^+$. Precursor ion: m/z 814. Product ions: m/z 375 ($[GdF_2(hmpa)]^+$, 50.49%), 505 ($[GdF(OTf)(hmpa)]^+$, 19.01%), 554 ($[GdF_2(hmpa)_2]^+$, 4.47%), 635 ($[Gd(OTf)_2(hmpa)]^+$, 15.73%), 684 ($[GdF(OTf)(hmpa)_2]^+$, 17.47%).

$[Tb(OTf)_2(hmpa)_2]^+$. Precursor ion: m/z 815. Product ions: m/z 376 ($[TbF_2(hmpa)]^+$, 61.09%), 506 ($[TbF(OTf)(hmpa)]^+$, 21.93%), 555 ($[TbF_2(hmpa)_2]^+$, 6.30%), 636 ($[Tb(OTf)_2(hmpa)]^+$, 19.76%), 685 ($[TbF(OTf)(hmpa)_2]^+$, 24.21%).

$[Dy(OTf)_2(hmpa)_2]^+$. Precursor ion: m/z 820. Product ions: m/z 381 ($[DyF_2(hmpa)]^+$, 9.41%), 511 ($[DyF(OTf)(hmpa)]^+$, 4.59%), 560 ($[DyF_2(hmpa)_2]^+$, 1.73%), 641 ($[Dy(OTf)_2(hmpa)]^+$, 5.20%), 690 ($[DyF(OTf)(hmpa)_2]^+$, 7.55%).

$[Ho(OTf)_2(hmpa)_2]^+$. Precursor ion: m/z 821. Product ions: m/z 382 ($[HoF_2(hmpa)]^+$, 34.01%), 512 ($[HoF(OTf)(hmpa)]^+$, 13.34%), 561 ($[HoF_2(hmpa)_2]^+$, 6.78%), 642 ($[Ho(OTf)_2(hmpa)]^+$, 14.27%), 691 ($[HoF(OTf)(hmpa)_2]^+$, 20.75%).

$[Er(OTf)_2(hmpa)_2]^+$. Precursor ion: m/z 824. Product ions: m/z 385 ($[ErF_2(hmpa)]^+$, 23.94%), 515 ($[ErF(OTf)(hmpa)]^+$, 9.17%), 564 ($[ErF_2(hmpa)_2]^+$, 5.42%), 645 ($[Er(OTf)_2(hmpa)]^+$, 10.56%), 694 ($[ErF(OTf)(hmpa)_2]^+$, 14.69%).

$[Tm(OTf)_2(hmpa)_2]^+$. Precursor ion: m/z 825. Product ions: m/z 386 ($[TmF_2(hmpa)]^+$, 20.83%), 516 ($[TmF(OTf)(hmpa)]^+$, 8.49%), 565 ($[TmF_2(hmpa)_2]^+$, 6.04%), 646 ($[Tm(OTf)_2(hmpa)]^+$, 10.81%), 695 ($[TmF(OTf)(hmpa)_2]^+$, 16.94%).

$[Yb(OTf)_2(hmpa)_2]^+$. Precursor ion: m/z 830. Product ions: m/z 391 ($[YbF_2(hmpa)]^+$, 24.51%), 521 ($[YbF(OTf)(hmpa)]^+$, 8.38%), 570 ($[YbF_2(hmpa)_2]^+$, 7.18%), 651 ($[Yb(OTf)_2(hmpa)]^+$, 8.51%), 700 ($[YbF(OTf)(hmpa)_2]^+$, 15.69%).

$[Lu(OTf)_2(hmpa)_2]^+$. Precursor ion: m/z 830. Product ions: m/z 392 ($[LuF_2(hmpa)]^+$, 63.53%), 522 ($[LuF(OTf)(hmpa)]^+$, 21.90%), 571 ($[LuF_2(hmpa)_2]^+$, 23.73%), 652 ($[Lu(OTf)_2(hmpa)]^+$, 23.73%), 701 ($[LuF(OTf)(hmpa)_2]^+$, 39.16%).

$[^{142}Nd(OTf)_2(hmpa)_2]^+$. Precursor ion: m/z 798. Product ions: m/z 359 ($[^{142}NdF_2(hmpa)]^+$, 58.34%), 489 ($[^{142}NdF(OTf)(hmpa)]^+$, 22.80%), 538 ($[^{142}NdF_2(hmpa)_2]^+$, 1.89%), 619 ($[^{142}Nd(OTf)_2(hmpa)]^+$, 19.92%), 668 ($[^{142}NdF(OTf)(hmpa)_2]^+$, 17.80%).

$[^{151}Eu(OTf)_2(hmpa)_2]^+$. Precursor ion: m/z 807. Product ions: m/z 349 ($[^{151}EuF(hmpa)]^+$, 31.21%), 368 ($[^{151}EuF_2(hmpa)]^+$, 50.57%), 479 ($[^{151}EuF(hmpa)]^+$, 47.43%), 498 ($[^{151}EuF(OTf)(hmpa)]^+$, 20.86%), 547 ($[^{151}EuF_2(hmpa)_2]^+$, 4.14%), 628 ($[^{151}Eu(OTf)_2(hmpa)]^+$, 21.51%), 658 ($[^{151}Eu(OTf)(hmpa)_2]^+$, 24.95%), 677 ($[^{151}EuF(OTf)(hmpa)_2]^+$, 24.95%).

$[^{166}Er(OTf)_2(hmpa)_2]^+$. Precursor ion: m/z 822. Product

ions: m/z 383 ($[^{166}ErF_2(hmpa)]^+$, 70.24%), 513 ($[^{166}ErF(OTf)(hmpa)]^+$, 36.39%), 562 ($[^{166}ErF_2(hmpa)_2]^+$, 24.36%), 643 ($[^{166}Er(OTf)_2(hmpa)]^+$, 40.43%), 692 ($[^{166}ErF(OTf)(hmpa)_2]^+$, 69.90%).

$[^{172}Yb(OTf)_2(hmpa)_2]^+$. Precursor ion: m/z 828. Product ions: m/z 389 ($[^{172}YbF_2(hmpa)]^+$, 35.08%), 519 ($[^{172}YbF(OTf)(hmpa)]^+$, 7.81%), 568 ($[^{172}YbF_2(hmpa)_2]^+$, 6.84%), 649 ($[^{172}Yb(OTf)_2(hmpa)]^+$, 7.30%), 698 ($[^{172}YbF(OTf)(hmpa)_2]^+$, 13.42%).

4.8.4. FAB(+)MS spectrum of tetrakis (hexamethylphosphoramide) rare earth(III) triflates. $[Sc(OTf)_2(tepo)_4]OTf$.

m/z 611 (100%), 745 (50%), 879 (1%).

$[Y(OTf)_2(tepo)_4]OTf$. m/z 655 (100%), 789 (84%), 923 (3%).

$[La(OTf)_2(tepo)_4]OTf$. m/z 705 (100%), 839 (65%).

$[Ce(OTf)_2(tepo)_4]OTf$. m/z 706 (100%), 840 (77%), 974 (2%).

$[Pr(OTf)_2(tepo)_4]OTf$. m/z 707 (100%), 841 (64%), 975 (1%).

$[Nd(OTf)_2(tepo)_4]OTf$. m/z 708 (^{142}Nd , 94%), 709 (^{143}Nd , 58%), 710 (^{144}Nd , 100%), 711 (^{145}Nd , 49%), 712 (^{146}Nd , 75%), 842 (^{142}Nd , 64%), 843 (^{143}Nd , 46%), 844 (^{144}Nd , 72%), 845 (^{145}Nd , 39%), 847 (^{146}Nd , 15%), 976 (^{142}Nd , 1%), 977 (^{143}Nd , 1%), 978 (^{144}Nd , 2%), 979 (^{145}Nd , 1%), 980 (^{146}Nd , 2%).

$[Sm(OTf)_2(tepo)_4]OTf$. m/z 713 (^{147}Sm , 54%), 714 (^{148}Sm , 50%), 715 (^{149}Sm , 60%), 716 (^{150}Sm , 44%), 718 (^{152}Sm , 100%), 720 (^{154}Sm , 88%), 847 (^{147}Sm , 39%), 848 (^{148}Sm , 38%), 849 (^{149}Sm , 46%), 850 (^{150}Sm , 33%), 852 (^{152}Sm , 71%), 854 (^{154}Sm , 65%), 983 (^{149}Sm , 1%), 986 (^{152}Sm , 2%), 988 (^{154}Sm , 1%).

$[Eu(OTf)_2(tepo)_4]OTf$. m/z 717 (^{151}Eu , 87%), 719 (^{153}Eu , 100%), 851 (^{151}Eu , 64%), 853 (^{153}Eu , 76%), 985 (^{151}Eu , 3%), 987 (^{153}Eu , 4%).

$[Gd(OTf)_2(tepo)_4]OTf$. m/z 720 (^{154}Gd , 12%), 721 (^{155}Gd , 52%), 722 (^{156}Gd , 79%), 723 (^{157}Gd , 68%), 724 (^{158}Gd , 100%), 726 (^{160}Gd , 81%), 854 (^{154}Gd , 34%), 855 (^{155}Gd , 34%), 856 (^{156}Gd , 53%), 857 (^{157}Gd , 49%), 858 (^{158}Gd , 67%), 860 (^{160}Gd , 53%), 990 (^{156}Gd , 1%), 991 (^{157}Gd , 1%), 992 (^{158}Gd , 2%), 994 (^{160}Gd , 1%).

$[Tb(OTf)_2(tepo)_4]OTf$. m/z 725 (100%), 859 (55%), 993 (1%).

$[Dy(OTf)_2(tepo)_4]OTf$. m/z 726 (^{160}Dy , 11%), 727 (^{161}Dy , 58%), 728 (^{162}Dy , 86%), 729 (^{163}Dy , 91%), 730 (^{164}Dy , 100%), 860 (^{160}Dy , 7%), 861 (^{161}Dy , 36%), 862 (^{162}Dy , 54%), 863 (^{163}Dy , 58%), 864 (^{164}Dy , 64%), 996 (^{162}Dy , 1%), 997 (^{163}Dy , 1%), 998 (^{164}Dy , 1%).

$[Ho(OTf)_2(tepo)_4]OTf$. m/z 731 (100%), 865 (68%), 999 (2%).

$[\text{Er}(\text{OTf})_2(\text{tepo})_4]\text{OTf}$. m/z 730 (^{164}Er , 11%), 732 (^{166}Er , 99%), 733 (^{167}Er , 81%), 734 (^{168}Er , 100%), 736 (^{170}Er , 55%), 864 (^{164}Er , 6%), 866 (^{166}Er , 75%), 867 (^{167}Er , 68%), 868 (^{168}Er , 80%), 870 (^{170}Er , 42%), 1000 (^{166}Er , 3%), 1001 (^{167}Er , 3%), 1002 (^{168}Er , 3%), 1004 (^{170}Er , 2%).

$[\text{Tm}(\text{OTf})_2(\text{tepo})_4]\text{OTf}$. m/z 735 (100%), 869 (56%), 1003 (1%).

$[\text{Yb}(\text{OTf})_2(\text{tepo})_4]\text{OTf}$. m/z 736 (^{170}Yb , 12%), 737 (^{171}Yb , 42%), 738 (^{172}Yb , 70%), 739 (^{173}Yb , 58%), 740 (^{174}Yb , 100%), 742 (^{176}Yb , 45%), 870 (^{170}Yb , 9%), 871 (^{171}Yb , 34%), 872 (^{172}Yb , 54%), 873 (^{173}Yb , 51%), 874 (^{174}Yb , 82%), 876 (^{176}Yb , 37%), 1005 (^{171}Yb , 1%), 1006 (^{172}Yb , 2%), 1007 (^{173}Yb , 3%), 1008 (^{174}Yb , 1%), 1010 (^{176}Yb , 1%).

$[\text{Lu}(\text{OTf})_2(\text{tepo})_4]\text{OTf}$. m/z 741 (100%), 875 (68%), 1009 (2%).

4.8.5. MS/MS spectra of precursor ions $[\text{M}(\text{OTf})_2(\text{tepo})_2]^+$. $[\text{Sc}(\text{OTf})_2(\text{tepo})_2]^+$. Precursor ion: m/z 611. Product ions: m/z 217 ($[\text{ScF}_2(\text{tepo})]^+$, 28.96%), 347 ($[\text{ScF}(\text{OTf})(\text{tepo})]^+$, 7.99%), 351 ($[\text{ScF}_2(\text{tepo})_2]^+$, 15.30%), 477 ($[\text{Sc}(\text{OTf})_2(\text{tepo})]^+$, 5.66%), 481 ($[\text{ScF}(\text{OTf})(\text{tepo})_2]^+$, 23.11%).

$[\text{Y}(\text{OTf})_2(\text{tepo})_2]^+$. Precursor ion: m/z 655. Product ions: m/z 261 ($[\text{YF}_2(\text{tepo})]^+$, 18.30%), 391 ($[\text{YF}(\text{OTf})(\text{tepo})]^+$, 10.22%), 395 ($[\text{YF}_2(\text{tepo})_2]^+$, 6.55%), 521 ($[\text{Y}(\text{OTf})_2(\text{tepo})]^+$, 9.67%), 525 ($[\text{YF}(\text{OTf})(\text{tepo})_2]^+$, 14.72%).

$[\text{La}(\text{OTf})_2(\text{tepo})_2]^+$. Precursor ion: m/z 705. Product ions: m/z 311 ($[\text{LaF}_2(\text{tepo})]^+$, 33.97%), 441 ($[\text{LaF}(\text{OTf})(\text{tepo})]^+$, 30.36%), 445 ($[\text{LaF}_2(\text{tepo})_2]^+$, 1.71%), 571 ($[\text{La}(\text{OTf})_2(\text{tepo})]^+$, 25.19%), 575 ($[\text{LaF}(\text{OTf})(\text{tepo})_2]^+$, 19.95%).

$[\text{Ce}(\text{OTf})_2(\text{tepo})_2]^+$. Precursor ion: m/z 706. Product ions: m/z 312 ($[\text{CeF}_2(\text{tepo})]^+$, 86.48%), 442 ($[\text{CeF}(\text{OTf})(\text{tepo})]^+$, 63.76%), 395 ($[\text{CeF}_2(\text{tepo})_2]^+$, 4.33%), 572 ($[\text{Ce}(\text{OTf})_2(\text{tepo})]^+$, 61.14%), 576 ($[\text{CeF}(\text{OTf})(\text{tepo})_2]^+$, 50.70%).

$[\text{Pr}(\text{OTf})_2(\text{tepo})_2]^+$. Precursor ion: m/z 707. Product ions: m/z 313 ($[\text{PrF}_2(\text{tepo})]^+$, 82.82%), 443 ($[\text{PrF}(\text{OTf})(\text{tepo})]^+$, 66.27%), 447 ($[\text{PrF}_2(\text{tepo})_2]^+$, 6.06%), 573 ($[\text{Pr}(\text{OTf})_2(\text{tepo})]^+$, 57.52%), 577 ($[\text{PrF}(\text{OTf})(\text{tepo})_2]^+$, 63.93%).

$[\text{Nd}(\text{OTf})_2(\text{tepo})_2]^+$. Precursor ion: m/z 710. Product ions: m/z 316 ($[\text{NdF}_2(\text{tepo})]^+$, 27.70%), 446 ($[\text{NdF}(\text{OTf})(\text{tepo})]^+$, 19.48%), 450 ($[\text{NdF}_2(\text{tepo})_2]^+$, 2.74%), 576 ($[\text{Nd}(\text{OTf})_2(\text{tepo})]^+$, 21.06%), 580 ($[\text{NdF}(\text{OTf})(\text{tepo})_2]^+$, 21.20%).

$[\text{Sm}(\text{OTf})_2(\text{tepo})_2]^+$. Precursor ion: m/z 718. Product ions: m/z 324 ($[\text{SmF}_2(\text{tepo})]^+$, 22.59%), 454 ($[\text{SmF}(\text{OTf})(\text{tepo})]^+$, 13.48%), 458 ($[\text{SmF}_2(\text{tepo})_2]^+$, 3. 17%), 584 ($[\text{Sm}(\text{OTf})_2(\text{tepo})]^+$, 15.57%), 688 ($[\text{SmF}(\text{OTf})(\text{tepo})_2]^+$, 16.85%).

$[\text{Eu}(\text{OTf})_2(\text{tepo})_2]^+$. Precursor ion: m/z 719. Product ions: m/z 306 ($[\text{EuF}(\text{tepo})]^+$, 14.76%), 325 ($[\text{EuF}_2(\text{tepo})]^+$, 14.97%), 436 ($[\text{Eu}(\text{OTf})(\text{tepo})]^+$, 34.97%), 455 ($[\text{EuF}(\text{OTf})(\text{tepo})]^+$, 8.39%), 459 ($[\text{EuF}_2(\text{tepo})_2]^+$, 3.49%), 570

($[\text{Eu}(\text{OTf})(\text{tepo})_2]^+$, 10.23%), 585 ($[\text{Eu}(\text{OTf})_2(\text{tepo})]^+$, 10.84%), 589 ($[\text{EuF}(\text{OTf})(\text{tepo})_2]^+$, 17.56%).

$[\text{Gd}(\text{OTf})_2(\text{tepo})_2]^+$. Pre cursor ion: m/z 724. Product ions: m/z 330 ($[\text{GdF}_2(\text{tepo})]^+$, 16.57%), 460 ($[\text{GdF}(\text{OTf})(\text{tepo})]^+$, 11.61%), 464 ($[\text{GdF}_2(\text{tepo})_2]^+$, 4. 19%), 590 ($[\text{Gd}(\text{OTf})_2(\text{tepo})]^+$, 16.44%), 594 ($[\text{GdF}(\text{OTf})(\text{tepo})_2]^+$, 17.19%).

$[\text{Tb}(\text{OTf})_2(\text{tepo})_2]^+$. Precursor ion: m/z 725. Product ions: m/z 331 ($[\text{TbF}_2(\text{tepo})]^+$, 33.20%), 461 ($[\text{TbF}(\text{OTf})(\text{tepo})]^+$, 16.67%), 465 ($[\text{TbF}_2(\text{tepo})_2]^+$, 7.02%), 591 ($[\text{Tb}(\text{OTf})_2(\text{tepo})]^+$, 16.40%), 595 ($[\text{TbF}(\text{OTf})(\text{tepo})_2]^+$, 20.06%).

$[\text{Dy}(\text{OTf})_2(\text{tepo})_2]^+$. Precursor ion: m/z 730. Product ions: m/z 336 ($[\text{DyF}_2(\text{tepo})]^+$, 38.27%), 466 ($[\text{DyF}(\text{OTf})(\text{tepo})]^+$, 22.14%), 470 ($[\text{DyF}_2(\text{tepo})_2]^+$, 11.02%), 596 ($[\text{Dy}(\text{OTf})_2(\text{tepo})]^+$, 28.53%), 600 ($[\text{DyF}(\text{OTf})(\text{tepo})_2]^+$, 36.51%).

$[\text{Ho}(\text{OTf})_2(\text{tepo})_2]^+$. Precursor ion: m/z 731. Product ions: m/z 337 ($[\text{HoF}_2(\text{tepo})]^+$, 53.01%), 467 ($[\text{HoF}(\text{OTf})(\text{tepo})]^+$, 27.82%), 471 ($[\text{HoF}_2(\text{tepo})_2]^+$, 17.33%), 597 ($[\text{Ho}(\text{OTf})_2(\text{tepo})]^+$, 34.40%), 601 ($[\text{HoF}(\text{OTf})(\text{tepo})_2]^+$, 45.97%).

$[\text{Er}(\text{OTf})_2(\text{tepo})_2]^+$. Precursor ion: m/z 734. Product ions: m/z 340 ($[\text{ErF}_2(\text{tepo})]^+$, 26.31%), 470 ($[\text{ErF}(\text{OTf})(\text{tepo})]^+$, 13.42%), 474 ($[\text{ErF}_2(\text{tepo})_2]^+$, 10.17%), 600 ($[\text{Er}(\text{OTf})_2(\text{tepo})]^+$, 16.91%), 604 ($[\text{ErF}(\text{OTf})(\text{tepo})_2]^+$, 23.42%).

$[\text{Tm}(\text{OTf})_2(\text{tepo})_2]^+$. Precursor ion: m/z 735. Product ions: m/z 341 ($[\text{TmF}_2(\text{tepo})]^+$, 54.27%), 471 ($[\text{TmF}(\text{OTf})(\text{tepo})]^+$, 28.14%), 566 ($[\text{TmF}_2(\text{tepo})_2]^+$, 22.26%), 601 ($[\text{Tm}(\text{OTf})_2(\text{tepo})]^+$, 35.14%), 605 ($[\text{TmF}(\text{OTf})(\text{tepo})_2]^+$, 49.12%).

$[\text{Yb}(\text{OTf})_2(\text{tepo})_2]^+$. Precursor ion: m/z 740. Product ions: m/z 346 ($[\text{YbF}_2(\text{tepo})]^+$, 48.48%), 476 ($[\text{YbF}(\text{OTf})(\text{tepo})]^+$, 26.03%), 480 ($[\text{YbF}_2(\text{tepo})_2]^+$, 23.48%), 606 ($[\text{Yb}(\text{OTf})_2(\text{tepo})]^+$, 30.30%), 610 ($[\text{YbF}(\text{OTf})(\text{tepo})_2]^+$, 48.56%).

$[\text{Lu}(\text{OTf})_2(\text{tepo})_2]^+$. Precursor ion: m/z 741. Product ions: m/z 347 ($[\text{LuF}_2(\text{tepo})]^+$, 99.54%), 477 ($[\text{LuF}(\text{OTf})(\text{tepo})]^+$, 48.91%), 481 ($[\text{LuF}_2(\text{tepo})_2]^+$, 49.69%), 607 ($[\text{Lu}(\text{OTf})_2(\text{tepo})]^+$, 62.78%), 611 ($[\text{LuF}(\text{OTf})(\text{tepo})_2]^+$, 86.74%).

4.8.6. FAB(+)MS spectrum of trimethyl phosphate-coordinated rare earth(III) triflates. Sc complex. m/z 623 (100%), 763 (15%), 903 (1%).

Y complex. m/z 666 (100%), 807 (26%).

La complex. m/z 717 (100%).

Ce complex. m/z 718 (100%).

Pr complex. m/z 719 (100%).

Nd complex. m/z 720 (^{142}Nd , 96%), 721 (^{143}Nd , 57%), 721 (^{144}Nd , 100%), 722 (^{145}Nd , 47%), 723 (^{146}Nd , 74%).

Sm complex. m/z 725 (^{147}Sm , 56%), 726 (^{148}Sm , 49%), 727 (^{149}Sm , 62%), 728 (^{150}Sm , 39%), 730 (^{152}Sm , 100%), 732 (^{154}Sm , 91%).

Eu complex. m/z 729 (^{151}Eu , 84%), 731 (^{153}Eu , 100%), 869 (^{151}Eu , 11%), 871 (^{153}Eu , 13%).

Gd complex. m/z 732 (^{154}Gd , 10%), 733 (^{155}Gd , 54%), 734 (^{156}Gd , 79%), 735 (^{157}Gd , 71%), 736 (^{158}Gd , 100%), 738 (^{160}Gd , 86%), 872 (^{154}Gd , 1%), 873 (^{155}Gd , 8%), 874 (^{156}Gd , 12%), 875 (^{157}Gd , 15%), 876 (^{158}Gd , 3%), 878 (^{160}Gd , 13%).

Tb complex. m/z 737 (100%), 877 (17%).

Dy complex. m/z 738 (^{160}Dy , 10%), 739 (^{161}Dy , 59%), 739 (^{162}Dy , 84%), 741 (^{163}Dy , 91%), 742 (^{164}Dy , 100%), 878 (^{160}Dy , 2%), 879 (^{161}Dy , 16%), 880 (^{162}Dy , 23%), 881 (^{163}Dy , 25%), 882 (^{164}Dy , 28%).

Ho complex. m/z 743 (100%), 883 (39%).

Er complex. m/z 742 (^{164}Er , 6%), 744 (^{166}Er , 100%), 745 (^{167}Er , 80%), 746 (^{168}Er , 97%), 748 (^{170}Er , 55%), 882 (^{164}Er , 2%), 884 (^{166}Er , 38%), 885 (^{167}Er , 31%), 886 (^{168}Er , 39%), 888 (^{170}Er , 21%).

Tm complex. m/z 747 (100%), 887 (23%).

Yb complex. m/z 748 (^{170}Yb , 11%), 749 (^{171}Yb , 42%), 750 (^{172}Yb , 67%), 751 (^{173}Yb , 59%), 752 (^{174}Yb , 100%), 754 (^{176}Yb , 47%), 888 (^{170}Yb , 5%), 889 (^{171}Yb , 19%), 890 (^{172}Yb , 31%), 891 (^{173}Yb , 27%), 892 (^{174}Yb , 47%), 894 (^{176}Yb , 22%).

Lu complex. m/z 753 (100%), 893 (21%).

4.8.7. MS/MS spectra of precursor ions $[\text{M}(\text{OTf})_2\text{tmp}]^+$. $[\text{Sc}(\text{OTf})_2(\text{tmp})_2]^+$. Precursor ion: m/z 623. Product ions: m/z 223 ($[\text{ScF}_2(\text{tmp})]^+$, 44.44%), 353 ($[\text{ScF}(\text{OTf})(\text{tmp})]^+$, 19.27%), 363 ($[\text{ScF}_2(\text{tmp})_2]^+$, 23.08%), 483 ($[\text{Sc}(\text{OTf})_2(\text{tmp})]^+$, 16.29%), 493 ($[\text{ScF}(\text{OTf})(\text{tmp})_2]^+$, 52.02%).

$[\text{Y}(\text{OTf})_2(\text{tmp})_2]^+$. Precursor ion: m/z 667. Product ions: m/z 267 ($[\text{YF}_2(\text{tmp})]^+$, 41.11%), 397 ($[\text{YF}(\text{OTf})(\text{tmp})]^+$, 28.8 1%), 407 ($[\text{YF}_2(\text{tmp})_2]^+$, 10.96%), 527 ($[\text{Y}(\text{OTf})_2(\text{tmp})]^+$, 25.33%), 536 ($[\text{YF}(\text{OTf})(\text{tmp})_2]^+$, 37.10%).

$[\text{La}(\text{OTf})_2(\text{tmp})_2]^+$. Precursor ion: m/z 717. Product ions: m/z 317 ($[\text{LaF}_2(\text{tmp})]^+$, 27.26%), 447 ($[\text{LaF}(\text{OTf})(\text{tmp})]^+$, 38. 10%), 457 ($[\text{LaF}_2(\text{tmp})_2]^+$, 0.71%), 577 ($[\text{LaF}(\text{OTf})_2(\text{tmp})]^+$, 24.51%), 587 ($[\text{LaF}(\text{OTf})(\text{tmp})_2]^+$, 13.95%).

$[\text{Ce}(\text{OTf})_2(\text{tmp})_2]^+$. Precursor ion: m/z 718. Product ions: m/z 318 ($[\text{CeF}_2(\text{tmp})]^+$, 62.07%), 448 ($[\text{CeF}(\text{OTf})(\text{tmp})]^+$, 63.65%), 458 ($[\text{CeF}_2(\text{tmp})_2]^+$, 1.55%), 578 ($[\text{Ce}(\text{OTf})_2(\text{tmp})]^+$, 44.40%), 588 ($[\text{CeF}(\text{OTf})(\text{tmp})_2]^+$, 32.92%).

$[\text{Pr}(\text{OTf})_2(\text{tmp})_2]^+$. Precursor ion: m/z 719. Product ions: m/z 319 ($[\text{PrF}_2(\text{tmp})]^+$, 71.09%), 449 ($[\text{PrF}(\text{OTf})(\text{tmp})]^+$, 77.31%), 459 ($[\text{PrF}_2(\text{tmp})_2]^+$, 2.42%), 579 ($[\text{PrF}(\text{OTf})_2(\text{tmp})]^+$, 44.60%), 589 ($[\text{PrF}(\text{OTf})(\text{tmp})_2]^+$, 38.28%).

$[\text{Nd}(\text{OTf})_2(\text{tmp})_2]^+$. Precursor ion: m/z 722. Product ions: m/z 322 ($[\text{NdF}_2(\text{tmp})]^+$, 40.36%), 452 ($[\text{NdF}(\text{OTf})(\text{tmp})]^+$,

43.25%), 462 ($[\text{NdF}_2(\text{tmp})_2]^+$, 2.40%), 582 ($[\text{Nd}(\text{OTf})_2(\text{tmp})]^+$, 29.24%), 592 ($[\text{NdF}(\text{OTf})(\text{tmp})_2]^+$, 28.22%).

$[\text{Sm}(\text{OTf})_2(\text{tmp})_2]^+$. Precursor ion: m/z 730. Product ions: m/z 330 ($[\text{SmF}_2(\text{tmp})]^+$, 36.85%), 460 ($[\text{SmF}(\text{OTf})(\text{tmp})]^+$, 36.09%), 470 ($[\text{SmF}_2(\text{tmp})_2]^+$, 3.66%), 590 ($[\text{Sm}(\text{OTf})_2(\text{tmp})]^+$, 27.88%), 600 ($[\text{SmF}(\text{OTf})(\text{tmp})_2]^+$, 29.44%).

$[\text{Eu}(\text{OTf})_2(\text{tmp})_2]^+$. Precursor ion: m/z 731. Product ions: m/z 312 ($[\text{EuF}(\text{tmp})]^+$, 11.17%), 331 ($[\text{EuF}_2(\text{tmp})]^+$, 16.82%), 441 ($[\text{Eu}(\text{OTf})(\text{tmp})]^+$, 38.76%), 461 ($[\text{EuF}(\text{OTf})(\text{tmp})]^+$, 9.14%), 471 ($[\text{EuF}_2(\text{tmp})_2]^+$, 2.69%), 582 ($[\text{Eu}(\text{OTf})(\text{tmp})_2]^+$, 11.02%), 591 ($[\text{Eu}(\text{OTf})_2(\text{tmp})]^+$, 17.15%), 601 ($[\text{EuF}(\text{OTf})(\text{tmp})_2]^+$, 21.60%).

$[\text{Gd}(\text{OTf})_2(\text{tmp})_2]^+$. Precursor ion: m/z 736. Product ions: m/z 336 ($[\text{GdF}_2(\text{tmp})]^+$, 10.28%), 566 ($[\text{GdF}(\text{OTf})(\text{tmp})]^+$, 9.02%), 476 ($[\text{GdF}_2(\text{tmp})_2]^+$, 1.85%), 596 ($[\text{Gd}(\text{OTf})_2(\text{tmp})]^+$, 9.54%), 606 ($[\text{GdF}(\text{OTf})(\text{tmp})_2]^+$, 10.13%).

$[\text{Tb}(\text{OTf})_2(\text{tmp})_2]^+$. Precursor ion: m/z 737. Product ions: m/z 337 ($[\text{TbF}_2(\text{tmp})]^+$, 23.07%), 467 ($[\text{TbF}(\text{OTf})(\text{tmp})]^+$, 18.17%), 477 ($[\text{TbF}_2(\text{tmp})_2]^+$, 4.27%), 597 ($[\text{Tb}(\text{OTf})_2(\text{tmp})]^+$, 15.80%), 606 ($[\text{TbF}(\text{OTf})(\text{tmp})_2]^+$, 21.53%).

$[\text{Dy}(\text{OTf})_2(\text{tmp})_2]^+$. Precursor ion: m/z 742. Product ions: m/z 342 ($[\text{DyF}_2(\text{tmp})]^+$, 24.24%), 472 ($[\text{DyF}(\text{OTf})(\text{tmp})]^+$, 20.06%), 482 ($[\text{DyF}_2(\text{tmp})_2]^+$, 5.82%), 602 ($[\text{Dy}(\text{OTf})_2(\text{tmp})]^+$, 19.30%), 612 ($[\text{DyF}(\text{OTf})(\text{tmp})_2]^+$, 27.11%).

$[\text{Ho}(\text{OTf})_2(\text{tmp})_2]^+$. Precursor ion: m/z 743. Product ions: m/z 343 ($[\text{HoF}_2(\text{tmp})]^+$, 27.40%), 473 ($[\text{HoF}(\text{OTf})(\text{tmp})]^+$, 20.49%), 483 ($[\text{HoF}_2(\text{tmp})_2]^+$, 8.16%), 603 ($[\text{Ho}(\text{OTf})_2(\text{tmp})]^+$, 21.82%), 613 ($[\text{HoF}(\text{OTf})(\text{tmp})_2]^+$, 31.30%).

$[\text{Er}(\text{OTf})_2(\text{tmp})_2]^+$. Precursor ion: m/z 744. Product ions: m/z 344 ($[\text{ErF}_2(\text{tmp})]^+$, 72.35%), 474 ($[\text{ErF}(\text{OTf})(\text{tmp})]^+$, 43.54%), 484 ($[\text{ErF}_2(\text{tmp})_2]^+$, 18.95%), 604 ($[\text{Er}(\text{OTf})_2(\text{tmp})]^+$, 40.24%), 614 ($[\text{ErF}(\text{OTf})(\text{tmp})_2]^+$, 57.11%).

$[\text{Tm}(\text{OTf})_2(\text{tmp})_2]^+$. Precursor ion: m/z 747. Product ions: m/z 347 ($[\text{TmF}_2(\text{tmp})]^+$, 28.39%), 477 ($[\text{TmF}(\text{OTf})(\text{tmp})]^+$, 20.26%), 487 ($[\text{TmF}_2(\text{tmp})_2]^+$, 10.03%), 607 ($[\text{Tm}(\text{OTf})_2(\text{tmp})]^+$, 22.54%), 617 ($[\text{TmF}(\text{OTf})(\text{tmp})_2]^+$, 32.81%).

$[\text{Yb}(\text{OTf})_2(\text{tmp})_2]^+$. Precursor ion: m/z 752. Product ions: m/z 352 ($[\text{YbF}_2(\text{tmp})]^+$, 16.27%), 482 ($[\text{YbF}(\text{OTf})(\text{tmp})]^+$, 12.24%), 492 ($[\text{YbF}_2(\text{tmp})_2]^+$, 6.70%), 612 ($[\text{Yb}(\text{OTf})_2(\text{tmp})]^+$, 13.49%), 622 ($[\text{YbF}(\text{OTf})(\text{tmp})_2]^+$, 21.99%).

$[\text{Lu}(\text{OTf})_2(\text{tmp})_2]^+$. Precursor ion: m/z 753. Product ions: m/z 353 ($[\text{LuF}_2(\text{tmp})]^+$, 22.81%), 483 ($[\text{LuF}(\text{OTf})(\text{tmp})]^+$, 19.43%), 493 ($[\text{LuF}_2(\text{tmp})_2]^+$, 12.53%), 613 ($[\text{Lu}(\text{OTf})_2(\text{tmp})]^+$, 22.35%), 623 ($[\text{LuF}(\text{OTf})(\text{tmp})_2]^+$, 30.72%).

4.8.8. FAB(+)MS spectra of hexakis(dimethylpropyl-eneurea) rare earth(III) triflate. Sc complex. m/z 599 (100%), 727 (29%).

Y complex. m/z 643 (100%), 771 (68%), 899 (4%).

La complex. m/z 693 (100%), 821 (47%).

Ce complex. m/z 694 (100%), 822 (71%).

Pr complex. m/z 695 (100%), 823 (68%).

Nd complex. m/z 696 (^{142}Nd , 93%), 697 (^{143}Nd , 62%), 698 (^{144}Nd , 100%), 699 (^{145}Nd , 54%), 700 (^{146}Nd , 78%), 824 (^{142}Nd , 44%), 825 (^{143}Nd , 32%), 826 (^{144}Nd , 50%), 827 (^{145}Nd , 29%), 828 (^{146}Nd , 38%).

Sm complex. m/z 701 (^{147}Sm , 44%), 702 (^{148}Sm , 42%), 703 (^{149}Sm , 50%), 704 (^{150}Sm , 35%), 706 (^{152}Sm , 81%), 708 (^{154}Sm , 73%), 829 (^{147}Sm , 11%), 830 (^{148}Sm , 11%), 831 (^{149}Sm , 14%), 832 (^{150}Sm , 10%), 834 (^{152}Sm , 20%), 836 (^{154}Sm , 19%).

Eu complex. m/z 705 (^{151}Eu , 63%), 707 (^{153}Eu , 75%), 833 (^{151}Eu , 12%), 835 (^{153}Eu , 14%).

Gd complex. m/z 708 (^{154}Gd , 12%), 709 (^{155}Gd , 53%), 710 (^{156}Gd , 79%), 711 (^{157}Gd , 72%), 712 (^{158}Gd , 100%), 714 (^{160}Gd , 87%), 836 (^{154}Gd , 7%), 837 (^{155}Gd , 34%), 838 (^{156}Gd , 52%), 839 (^{157}Gd , 50%), 840 (^{158}Gd , 67%), 842 (^{160}Gd , 55%).

Tb complex. m/z 713 (100%), 841 (23%).

Dy complex. m/z 714 (^{160}Dy , 11%), 715 (^{161}Dy , 58%), 716 (^{162}Dy , 85%), 717 (^{163}Dy , 91%), 718 (^{164}Dy , 100%), 843 (^{161}Dy , 25%), 844 (^{162}Dy , 38%), 845 (^{163}Dy , 41%), 846 (^{164}Dy , 46%).

Ho complex. m/z 719 (100%), 847 (31%).

Er complex. m/z 718 (^{164}Er , 7%), 720 (^{166}Er , 99%), 721 (^{167}Er , 85%), 722 (^{168}Er , 100%), 724 (^{170}Er , 56%), 848 (^{166}Er , 31%), 849 (^{167}Er , 29%), 850 (^{168}Er , 33%), 852 (^{170}Er , 17%).

Tm complex. m/z 723 (100%), 851 (45%).

Yb complex. m/z 724 (^{170}Yb , 10%), 725 (^{171}Yb , 41%), 726 (^{172}Yb , 8%), 727 (^{173}Yb , 59%), 728 (^{174}Yb , 100%), 730 (^{176}Yb , 46%), 853 (^{171}Yb , 16%), 854 (^{172}Yb , 26%), 855 (^{173}Yb , 23%), 856 (^{174}Yb , 38%), 858 (^{176}Yb , 17%).

Lu complex. m/z 729 (100%), 857 (48%).

4.8.9. MS/MS spectra of precursor ions $[\text{M}(\text{OTf})_2(\text{dmpu})_2]^+$. $[\text{Sc}(\text{OTf})_2(\text{dmpu})_2]^+$. Precursor ion: m/z 599. Product ions: m/z 211 ($[\text{ScF}_2(\text{dmpu})]^+$, 55.10%), 339 ($[\text{ScF}_2(\text{dmpu})_2]^+$, 9.64%), 341 ($[\text{ScF}(\text{OTf})(\text{dmpu})]^+$, 16.29%), 469 ($[\text{ScF}(\text{OTf})(\text{dmpu})]^+$, 24.95%), 471 ($[\text{Sc}(\text{OTf})_2(\text{dmpu})]^+$, 15.03%).

$[\text{Y}(\text{OTf})_2(\text{dmpu})_2]^+$. Precursor ion: m/z 643. Product ions: m/z 255 ($[\text{YF}_2(\text{dmpu})]^+$, 80.60%), 383 ($[\text{YF}_2(\text{dmpu})_2]^+$, 10.34%), 385 ($[\text{YF}(\text{OTf})(\text{dmpu})]^+$, 47.17%), 513 ($[\text{YF}(\text{OTf})(\text{dmpu})_2]^+$, 36.78%), 515 ($[\text{Y}(\text{OTf})_2(\text{dmpu})]^+$, 43.57%).

$[\text{La}(\text{OTf})_2(\text{dmpu})_2]^+$. Precursor ion: m/z 693. Product ions: m/z 305 ($[\text{LaF}_2(\text{dmpu})]^+$, 36.60%), 433 ($[\text{LaF}_2(\text{dmpu})_2]^+$, 3.57%), 435 ($[\text{LaF}(\text{OTf})(\text{dmpu})]^+$, 38.70%), 563

($[\text{LaF}(\text{OTf})(\text{dmpu})_2]^+$, 11.22%), 565 ($[\text{La}(\text{OTf})_2(\text{dmpu})]^+$, 40.91%).

$[\text{Ce}(\text{OTf})_2(\text{dmpu})_2]^+$. Precursor ion: m/z 694. Product ions: m/z 306 ($[\text{CeF}_2(\text{dmpu})]^+$, 52.29%), 434 ($[\text{CeF}_2(\text{dmpu})_2]^+$, 2.48%), 436 ($[\text{CeF}(\text{OTf})(\text{dmpu})]^+$, 48.93%), 564 ($[\text{CeF}(\text{OTf})(\text{dmpu})_2]^+$, 14.17%), 566 ($[\text{Ce}(\text{OTf})_2(\text{dmpu})]^+$, 44.99%).

$[\text{Pr}(\text{OTf})_2(\text{dmpu})_2]^+$. Precursor ion: m/z 695. Product ions: m/z 307 ($[\text{PrF}_2(\text{dmpu})]^+$, 57.77%), 9.64%), 435 ($[\text{PrF}_2(\text{dmpu})_2]^+$, 4.87%), 437 ($[\text{PrF}(\text{OTf})(\text{dmpu})]^+$, 48.85%), 565 ($[\text{PrF}(\text{OTf})(\text{dmpu})_2]^+$, 17.13%), 567 ($[\text{Pr}(\text{OTf})_2(\text{dmpu})]^+$, 40.47%).

$[\text{Nd}(\text{OTf})_2(\text{dmpu})_2]^+$. Precursor ion: m/z 698. Product ions: m/z 310 ($[\text{NdF}_2(\text{dmpu})]^+$, 19.30%), 438 ($[\text{NdF}_2(\text{dmpu})_2]^+$, 2.51%), 440 ($[\text{NdF}(\text{OTf})(\text{dmpu})]^+$, 14.63%), 568 ($[\text{NdF}(\text{OTf})(\text{dmpu})_2]^+$, 7.26%), 570 ($[\text{Nd}(\text{OTf})_2(\text{dmpu})]^+$, 16.27%).

$[\text{Sm}(\text{OTf})_2(\text{dmpu})_2]^+$. Precursor ion: m/z 706. Product ions: m/z 318 ($[\text{SmF}_2(\text{dmpu})]^+$, 27.85%), 446 ($[\text{SmF}_2(\text{dmpu})_2]^+$, 2.65%), 448 ($[\text{SmF}(\text{OTf})(\text{dmpu})]^+$, 18.50%), 576 ($[\text{SmF}(\text{OTf})(\text{dmpu})_2]^+$, 10.85%), 578 ($[\text{SmF}(\text{OTf})_2(\text{dmpu})]^+$, 21.19%).

$[\text{Eu}(\text{OTf})_2(\text{dmpu})_2]^+$. Precursor ion: m/z 707. Product ions: m/z 300 ($[\text{EuF}(\text{dmpu})]^+$, 8.09%), 319 ($[\text{EuF}_2(\text{dmpu})]^+$, 21.53%), 430 ($[\text{Eu}(\text{OTf})(\text{dmpu})]^+$, 18.23%), 447 ($[\text{EuF}_2(\text{dmpu})_2]^+$, 1.69%), 449 ($[\text{EuF}(\text{OTf})(\text{dmpu})]^+$, 17.15%), 558 ($[\text{Eu}(\text{OTf})(\text{dmpu})_2]^+$, 10.70%), 577 ($[\text{EuF}(\text{OTf})(\text{dmpu})_2]^+$, 10.91%), 579 ($[\text{Eu}(\text{OTf})_2(\text{dmpu})]^+$, 19.98%).

$[\text{Gd}(\text{OTf})_2(\text{dmpu})_2]^+$. Precursor ion: m/z 712. Product ions: m/z 324 ($[\text{GdF}_2(\text{dmpu})]^+$, 14.30%), 452 ($[\text{GdF}_2(\text{dmpu})_2]^+$, 2.05%), 454 ($[\text{GdF}(\text{OTf})(\text{dmpu})]^+$, 9.21%), 582 ($[\text{GdF}(\text{OTf})(\text{dmpu})_2]^+$, 6.63%), 584 ($[\text{Gd}(\text{OTf})_2(\text{dmpu})]^+$, 14.74%).

$[\text{Tb}(\text{OTf})_2(\text{dmpu})_2]^+$. Precursor ion: m/z 713. Product ions: m/z 325 ($[\text{TbF}_2(\text{dmpu})]^+$, 63.70%), 453 ($[\text{TbF}_2(\text{dmpu})_2]^+$, 5.93%), 455 ($[\text{TbF}(\text{OTf})(\text{dmpu})]^+$, 35.40%), 583 ($[\text{TbF}(\text{OTf})(\text{dmpu})_2]^+$, 27.39%), 585 ($[\text{TbF}(\text{OTf})_2(\text{dmpu})]^+$, 35.60%).

$[\text{Dy}(\text{OTf})_2(\text{dmpu})_2]^+$. Precursor ion: m/z 718. Product ions: m/z 330 ($[\text{DyF}_2(\text{dmpu})]^+$, 19.99%), 458 ($[\text{DyF}_2(\text{dmpu})_2]^+$, 3.17%), 460 ($[\text{DyF}(\text{OTf})(\text{dmpu})]^+$, 11.66%), 588 ($[\text{DyF}(\text{OTf})(\text{dmpu})_2]^+$, 10.59%), 560 ($[\text{DyF}(\text{OTf})_2(\text{dmpu})]^+$, 14.70%).

$[\text{Ho}(\text{OTf})_2(\text{dmpu})_2]^+$. Precursor ion: m/z 719. Product ions: m/z 331 ($[\text{HoF}_2(\text{dmpu})]^+$, 78.07%), 459 ($[\text{HoF}_2(\text{dmpu})_2]^+$, 9.89%), 461 ($[\text{HoF}(\text{OTf})(\text{dmpu})]^+$, 40.14%), 589 ($[\text{HoF}(\text{OTf})(\text{dmpu})_2]^+$, 37.36%), 591 ($[\text{Ho}(\text{OTf})_2(\text{dmpu})]^+$, 50.63%).

$[\text{Er}(\text{OTf})_2(\text{dmpu})_2]^+$. Precursor ion: m/z 722. Product ions: m/z 334 ($[\text{ErF}_2(\text{dmpu})]^+$, 27.19%), 462 ($[\text{ErF}_2(\text{dmpu})_2]^+$, 4.89%), 464 ($[\text{ErF}(\text{OTf})(\text{dmpu})]^+$, 16.54%), 592 ($[\text{ErF}(\text{OTf})(\text{dmpu})_2]^+$, 15.59%), 594 ($[\text{ErF}(\text{OTf})_2(\text{dmpu})]^+$, 21.81%).

$[Tm(OTf)_2(dmpu)_2]^+$. Precursor ion: m/z 723. Product ions: m/z 335 ($[TmF_2(dmpu)]^+$, 92.76%), 463 ($[TmF_2(dmpu)_2]^+$, 11.38%), 465 ($[TmF(OTf)(dmpu)]^+$, 39.82%), 593 ($[TmF(OTf)(dmpu)_2]^+$, 34.41%), 595 ($[TmF(OTf)_2(dmpu)]^+$, 42.00%).

$[Yb(OTf)_2(dmpu)_2]^+$. Precursor ion: m/z 728. Product ions: m/z 340 ($[YbF_2(dmpu)]^+$, 22.62%), 468 ($[YbF_2(dmpu)_2]^+$, 4.77%), 470 ($[YbF(OTf)(dmpu)]^+$, 11.45%), 598 ($[YbF(OTf)(dmpu)_2]^+$, 15.64%), 600 ($[YbF(OTf)_2(dmpu)]^+$, 18.65%).

$[Lu(OTf)_2(dmpu)_2]^+$. Precursor ion: m/z 729. Product ions: m/z 341 ($[LuF_2(dmpu)]^+$, 91.64%), 469 ($[LuF_2(dmpu)_2]^+$, 14.43%), 471 ($[LuF(OTf)(dmpu)]^+$, 36.24%), 599 ($[LuF(OTf)(dmpu)_2]^+$, 33.05%), 601 ($[LuF(OTf)_2(dmpu)]^+$, 41.73%).

4.8.10. FAB(+)MS spectra of dimethyl sulfoxide-coordinated rare earth(III) triflate. Sc complex. m/z 499 (100%), 577 (37%), 655 (4%).

Y complex. m/z 543 (100%), 621 (57%).

La complex. m/z 593 (100%), 671 (36%).

Ce complex. m/z 594 (100%), 672 (17%).

Pr complex. m/z 595 (100%), 673 (78%).

Nd complex. m/z 596 (^{142}Nd , 90%), 597 (^{143}Nd , 50%), 598 (^{144}Nd , 100%), 599 (^{145}Nd , 56%), 600 (^{146}Nd , 76%), 674 (^{142}Nd , 16%), 675 (^{143}Nd , 9%), 676 (^{144}Nd , 18%), 677 (^{145}Nd , 9%), 678 (^{146}Nd , 15%).

Sm complex. m/z 601 (^{147}Sm , 53%), 602 (^{148}Sm , 45%), 603 (^{149}Sm , 63%), 604 (^{150}Sm , 40%), 606 (^{152}Sm , 100%), 608 (^{154}Sm , 96%), 679 (^{147}Sm , 20%), 680 (^{148}Sm , 18%), 681 (^{149}Sm , 25%), 682 (^{150}Sm , 16%), 684 (^{152}Sm , 34%), 686 (^{154}Sm , 38%).

Eu complex. m/z 605 (^{151}Eu , 78%), 607 (^{153}Eu , 100%), 683 (^{151}Eu , 51%), 685 (^{153}Eu , 67%).

Gd complex. m/z 608 (^{154}Gd , 7%), 609 (^{155}Gd , 49%), 610 (^{156}Gd , 72%), 611 (^{157}Gd , 67%), 612 (^{158}Gd , 100%), 614 (^{160}Gd , 89%), 686 (^{154}Gd , 4%), 687 (^{155}Gd , 26%), 688 (^{156}Gd , 39%), 689 (^{157}Gd , 38%), 690 (^{158}Gd , 55%), 692 (^{160}Gd , 49%).

Tb complex. m/z 613 (100%), 691 (45%).

Dy complex. m/z 614 (^{160}Dy , 7%), 615 (^{161}Dy , 52%), 616 (^{162}Dy , 77%), 617 (^{163}Dy , 84%), 618 (^{164}Dy , 100%), 693 (^{161}Dy , 41%), 694 (^{162}Dy , 59%), 695 (^{163}Dy , 49%), 696 (^{164}Dy , 80%).

Ho complex. m/z 619 (100%), 697 (38%).

Er complex. m/z 618 (^{164}Er , 5%), 620 (^{166}Er , 95%), 621 (^{167}Er , 74%), 622 (^{168}Er , 100%), 624 (^{170}Er , 62%), 698 (^{166}Er , 68%), 699 (^{167}Er , 56%), 700 (^{168}Er , 76%), 702 (^{170}Er , 47%).

Tm complex. m/z 623 (100%), 701 (59%).

Yb complex. m/z 624 (^{170}Yb , 8%), 625 (^{171}Yb , 39%), 626 (^{172}Yb , 63%), 627 (^{173}Yb , 56%), 628 (^{174}Yb , 100%), 630 (^{176}Yb , 53%), 703 (^{171}Yb , 11%), 704 (^{172}Yb , 19%), 705 (^{173}Yb , 17%), 706 (^{174}Yb , 30%), 708 (^{176}Yb , 16%).

Lu complex. m/z 629 (100%), 707 (48%).

4.8.11. MS/MS spectra of $[\text{M}(\text{OTf})_2(\text{dmso})_2]^+$. $[\text{Sc}(\text{OTf})_2(\text{dmso})_2]^+$. Precursor ion: m/z 499. Product ions: m/z 161 ($[\text{Sc}_2(\text{dmso})]^+$, 11.06%), 239 ($[\text{ScF}_2(\text{dmso})_2]^+$, 4.41%), 291 ($[\text{ScF}(\text{OTf})(\text{dmso})]^+$, 11.74%), 369 ($[\text{ScF}(\text{OTf})(\text{dmso})_2]^+$, 14.95%), 421 ($[\text{Sc}(\text{OTf})_2(\text{dmso})]^+$, 15.65%).

$[\text{Y}(\text{OTf})_2(\text{dmso})_2]^+$. Precursor ion: m/z 543. Product ions: m/z 205 ($[\text{YF}_2(\text{dmso})]^+$, 9.41%), 283 ($[\text{YF}_2(\text{dmso})_2]^+$, 2.76%), 335 ($[\text{YF}(\text{OTf})(\text{dmso})]^+$, 16.70%), 413 ($[\text{YF}(\text{OTf})(\text{dmso})_2]^+$, 13.36%), 465 ($[\text{Y}(\text{OTf})_2(\text{dmso})]^+$, 20.59%).

$[\text{La}(\text{OTf})_2(\text{dmso})_2]^+$. Precursor ion: m/z 593. Product ions: m/z 255 ($[\text{LaF}_2(\text{dmso})]^+$, 8.74%), 333 ($[\text{LaF}_2(\text{dmso})_2]^+$, 0.39%), 385 ($[\text{LaF}(\text{OTf})(\text{dmso})]^+$, 23.18%), 463 ($[\text{LaF}(\text{OTf})(\text{dmso})_2]^+$, 6.97%), 515 ($[\text{La}(\text{OTf})_2(\text{dmso})]^+$, 31.45%).

$[\text{Ce}(\text{OTf})_2(\text{dmso})_2]^+$. Precursor ion: m/z 594. Product ions: m/z 256 ($[\text{CeF}_2(\text{dmso})]^+$, 11.51%), 334 ($[\text{CeF}_2(\text{dmso})_2]^+$, 0.48%), 386 ($[\text{CeF}(\text{OTf})(\text{dmso})]^+$, 29.03%), 464 ($[\text{CeF}(\text{OTf})(\text{dmso})_2]^+$, 9.99%), 516 ($[\text{Ce}(\text{OTf})_2(\text{dmso})]^+$, 34.66%).

$[\text{Pr}(\text{OTf})_2(\text{dmso})_2]^+$. Precursor ion: m/z 595. Product ions: m/z 257 ($[\text{PrF}_2(\text{dmso})]^+$, 10.32%), 9.64%), 335 ($[\text{PrF}_2(\text{dmso})_2]^+$, 0.55%), 387 ($[\text{PrF}(\text{OTf})(\text{dmso})]^+$, 23.05%), 465 ($[\text{PrF}(\text{OTf})(\text{dmso})_2]^+$, 8.18%), 517 ($[\text{Pr}(\text{OTf})_2(\text{dmso})]^+$, 27.07%).

$[\text{Nd}(\text{OTf})_2(\text{dmso})_2]^+$. Precursor ion: m/z 598. Product ions: m/z 260 ($[\text{NdF}_2(\text{dmso})]^+$, 9.93%), 338 ($[\text{NdF}_2(\text{dmso})_2]^+$, 0.76%), 390 ($[\text{NdF}(\text{OTf})(\text{dmso})]^+$, 22.66%), 468 ($[\text{NdF}(\text{OTf})(\text{dmso})_2]^+$, 11.09%), 520 ($[\text{Nd}(\text{OTf})_2(\text{dmso})]^+$, 30.36%).

$[\text{Sm}(\text{OTf})_2(\text{dmso})_2]^+$. Precursor ion: m/z 606. Product ions: m/z 268 ($[\text{SmF}_2(\text{dmso})]^+$, 11.99%), 346 ($[\text{SmF}_2(\text{dmso})_2]^+$, 1.40%), 398 ($[\text{SmF}(\text{OTf})(\text{dmso})]^+$, 24.69%), 476 ($[\text{SmF}(\text{OTf})(\text{dmso})_2]^+$, 13.51%), 528 ($[\text{SmF}(\text{OTf})_2(\text{dmso})]^+$, 34.00%).

$([\text{Eu}(\text{OTf})(\text{dmso})_2]^+)$. Precursor ion: m/z 607. Product ions: m/z 250 ($[\text{EuF}(\text{dmso})]^+$, 8.11%), 269 ($[\text{EuF}_2(\text{dmso})]^+$, 13.27%), 347 ($[\text{EuF}_2(\text{dmso})_2]^+$, 1.99%), 380 ($[\text{Eu}(\text{OTf})(\text{dmso})]^+$, 28.95%), 399 ($[\text{EuF}(\text{OTf})(\text{dmso})]^+$, 30.14%), 458 ($[\text{Eu}(\text{OTf})(\text{dmso})_2]^+$, 13.09%), 477 ($[\text{EuF}(\text{OTf})(\text{dmso})_2]^+$, 17.88%), 529 ($[\text{Eu}(\text{OTf})_2(\text{dmso})]^+$, 42.28%).

$[\text{Gd}(\text{OTf})_2(\text{dmso})_2]^+$. Precursor ion: m/z 612. Product ions: m/z 274 ($[\text{GdF}_2(\text{dmso})]^+$, 13.96%), 352 ($[\text{GdF}_2(\text{dmso})_2]^+$, 2.48%), 404 ($[\text{GdF}(\text{OTf})(\text{dmso})]^+$, 26. 86%), 482

$[\text{GdF}(\text{OTf})(\text{dmso})_2]^+$, 18.44%), 534 ($[\text{Gd}(\text{OTf})_2(\text{dmso})]^+$, 45.54%).

$[\text{Tb}(\text{OTf})_2(\text{dmso})_2]^+$. Precursor ion: m/z 613. Product ions: m/z 275 ($[\text{TbF}_2(\text{dmso})]^+$, 18.46%), 353 ($[\text{TbF}_2(\text{dmso})_2]^+$, 3.38%), 405 ($[\text{TbF}(\text{OTf})(\text{dmso})]^+$, 29.48%), 483 ($[\text{TbF}(\text{OTf})(\text{dmso})_2]^+$, 20.86%), 535 ($[\text{Tb}(\text{OTf})_2(\text{dmso})]^+$, 40.38%).

$[\text{Dy}(\text{OTf})_2(\text{dmso})_2]^+$. Precursor ion: m/z 618. Product ions: m/z 280 ($[\text{DyF}_2(\text{dmso})_2]^+$, 8.77%), 358 ($[\text{DyF}_2(\text{dmso})_2]^+$, 2.09%), 410 ($[\text{DyF}(\text{OTf})(\text{dmso})]^+$, 14.19%), 488 ($[\text{DyF}(\text{OTf})(\text{dmso})_2]^+$, 11.24%), 540 ($[\text{Dy}(\text{OTf})_2(\text{dmso})]^+$, 19.00%).

$[\text{Ho}(\text{OTf})_2(\text{dmso})_2]^+$. Precursor ion: m/z 619. Product ions: m/z 281 ($[\text{HoF}_2(\text{dmso})]^+$, 9.16%), 359 ($[\text{HoF}_2(\text{dmso})_2]^+$, 5.81%), 411 ($[\text{HoF}(\text{OTf})(\text{dmso})]^+$, 34.89%), 489 ($[\text{HoF}(\text{OTf})(\text{dmso})_2]^+$, 28.34%), 541 ($[\text{Ho}(\text{OTf})_2(\text{dmso})]^+$, 49.15%).

$[\text{Er}(\text{OTf})_2(\text{dmso})_2]^+$. Precursor ion: m/z 622. Product ions: m/z 284 ($[\text{ErF}_2(\text{dmso})]^+$, 13.31%), 362 ($[\text{ErF}_2(\text{dmso})_2]^+$, 4.28%), 414 ($[\text{ErF}(\text{OTf})(\text{dmso})]^+$, 20.81%), 492 ($[\text{ErF}(\text{OTf})(\text{dmso})_2]^+$, 19.56%), 544 ($[\text{Er}(\text{OTf})_2(\text{dmso})]^+$, 3.1.77%).

$[\text{Tm}(\text{OTf})_2(\text{dmso})_2]^+$. Precursor ion: m/z 623. Product ions: m/z 285 ($[\text{TmF}_2(\text{dmso})]^+$, 18.04%), 363 ($[\text{TmF}_2(\text{dmso})_2]^+$, 5.85%), 415 ($[\text{TmF}(\text{OTf})(\text{dmso})]^+$, 26.15%), 493 ($[\text{TmF}(\text{dmso})_2]^+$, 23.83%), 545 ($[\text{Tm}(\text{OTf})_2(\text{dmso})]^+$, 38.02%).

$[\text{Yb}(\text{OTf})_2(\text{dmso})_2]^+$. Precursor ion: m/z 628. Product ions: m/z 290 ($[\text{YbF}_2(\text{dmso})]^+$, 8.31%), 368 ($[\text{YbF}_2(\text{dmso})_2]^+$, 3.08%), 420 ($[\text{YbF}(\text{OTf})(\text{dmso})]^+$, 12.57%), 498 ($[\text{YbF}(\text{OTf})(\text{dmso})_2]^+$, 12.21%), 550 ($[\text{Yb}(\text{OTf})_2(\text{dmso})]^+$, 15.49%).

$[\text{Lu}(\text{OTf})_2(\text{dmso})_2]^+$. Precursor ion: m/z 629. Product ions: m/z 291 ($[\text{LuF}_2(\text{dmso})]^+$, 26.04%), 369 ($[\text{LuF}_2(\text{dmso})]^+$, 10.00%), 421 ($[\text{LuF}(\text{OTf})(\text{dmso})]^+$, 35. 80%), 499 ($[\text{LuF}(\text{OTf})(\text{dmso})_2]^+$, 33.56%), 551 ($[\text{LuF}(\text{OTf})_2(\text{dmso})]^+$, 50.49%).

4.8.12. MS/MS spectra of $[\text{M}(\text{OTf})_2(\text{tepo})_4]^+$. $[\text{Sc}(\text{OTf})_2(\text{tepo})_4]^+$. Precursor ion: m/z 879. Product ions: m/z 611 ($[\text{Sc}(\text{OTf})_2(\text{tepo})_2]^+$, 10.28%), 745 ($[\text{Sc}(\text{OTf})_2(\text{tepo})_3]^+$, 48.62%).

$[\text{Y}(\text{OTf})_2(\text{tepo})_4]^+$. Precursor ion: m/z 923. Product ions: m/z 655 ($[\text{Y}(\text{OTf})_2(\text{tepo})_2]^+$, 13.87%), 789 ($[\text{Y}(\text{OTf})_2(\text{tepo})_3]^+$, 59.37%).

$[\text{La}(\text{OTf})_2(\text{tepo})_4]^+$. Precursor ion: m/z 973. Product ions: m/z 705 ($[\text{La}(\text{OTf})_2(\text{tepo})_2]^+$, 15.21%), 839 ($[\text{La}(\text{OTf})_2(\text{tepo})_3]^+$, 61.80%).

$[\text{Ce}(\text{OTf})_2(\text{tepo})_4]^+$. Precursor ion: m/z 974. Product ions: m/z 706 ($[\text{Ce}(\text{OTf})_2(\text{tepo})_2]^+$, 7.01%), 840 ($[\text{Ce}(\text{OTf})_2(\text{tepo})_3]^+$, 29.11%).

$[\text{Pr}(\text{OTf})_2(\text{tepo})_4]^+$. Precursor ion: m/z 975. Product ions:

m/z 707 ($[\text{Pr}(\text{OTf})_2(\text{tepo})_2]^+$, 11.80%), 841 ($[\text{Pr}(\text{OTf})_2(\text{tepo})_3]^+$, 48.88%).

$[\text{Nd}(\text{OTf})_2(\text{tepo})_4]^+$. Precursor ion: m/z 978. Product ions: m/z 710 ($[\text{Nd}(\text{OTf})_2(\text{tepo})_2]^+$, 17.06%), 843 ($[\text{Nd}(\text{OTf})_2(\text{tepo})_3]^+$, 69.30%).

$[\text{Sm}(\text{OTf})_2(\text{tepo})_4]^+$. Precursor ion: m/z 986. Product ions: m/z 718 ($[\text{Sm}(\text{OTf})_2(\text{tepo})_2]^+$, 6.48%), 851 ($[\text{Sm}(\text{OTf})_2(\text{tepo})_3]^+$, 27.07%).

$[\text{Eu}(\text{OTf})_2(\text{tepo})_4]^+$. Precursor ion: m/z 987. Product ions: m/z 719 ($[\text{Eu}(\text{OTf})_2(\text{tepo})_2]^+$, 12.50%), 852 ($[\text{Eu}(\text{OTf})_2(\text{tepo})_3]^+$, 53.48%).

$[\text{Gd}(\text{OTf})_2(\text{tepo})_4]^+$. Precursor ion: m/z 992. Product ions: m/z 724 ($[\text{Gd}(\text{OTf})_2(\text{tepo})_2]^+$, 9.34%), 858 ($[\text{Gd}(\text{OTf})_2(\text{tepo})_3]^+$, 38.60%).

$[\text{Tb}(\text{OTf})_2(\text{tepo})_4]^+$. Precursor ion: m/z 993. Product ions: m/z 725 ($[\text{Tb}(\text{OTf})_2(\text{tepo})_2]^+$, 8.27%), 859 ($[\text{Tb}(\text{OTf})_2(\text{tepo})_3]^+$, 34.69%).

$[\text{Dy}(\text{OTf})_2(\text{tepo})_4]^+$. Precursor ion: m/z 998. Product ions: m/z 730 ($[\text{Dy}(\text{OTf})_2(\text{tepo})_2]^+$, 6.58%), 864 ($[\text{Dy}(\text{OTf})_2(\text{tepo})_3]^+$, 28.32%).

$[\text{Ho}(\text{OTf})_2(\text{tepo})_4]^+$. Precursor ion: m/z 999. Product ions: m/z 731 ($[\text{Ho}(\text{OTf})_2(\text{tepo})_2]^+$, 20.07%), 865 ($[\text{Ho}(\text{OTf})_2(\text{tepo})_3]^+$, 83.49%).

$[\text{Er}(\text{OTf})_2(\text{tepo})_4]^+$. Precursor ion: m/z 1002. Product ions: m/z 734 ($[\text{Er}(\text{OTf})_2(\text{tepo})_2]^+$, 6.94%), 868 ($[\text{Er}(\text{OTf})_2(\text{tepo})_3]^+$, 28.99%).

$[\text{Tm}(\text{OTf})_2(\text{tepo})_4]^+$. Precursor ion: m/z 1003. Product ions: m/z 735 ($[\text{Tm}(\text{OTf})_2(\text{tepo})_2]^+$, 13.10%), 869 ($[\text{Tm}(\text{OTf})_2(\text{tepo})_3]^+$, 55.92%).

$[\text{Yb}(\text{OTf})_2(\text{tepo})_4]^+$. Precursor ion: m/z 1008. Product ions: m/z 740 ($[\text{Yb}(\text{OTf})_2(\text{tepo})_2]^+$, 11.58%), 874 ($[\text{Yb}(\text{OTf})_2(\text{tepo})_3]^+$, 52.94%).

$[\text{Lu}(\text{OTf})_2(\text{tepo})_4]^+$. Precursor ion: m/z 1009. Product ions: m/z 741 ($[\text{Lu}(\text{OTf})_2(\text{tepo})_2]^+$, 11.67%), 885 ($[\text{Lu}(\text{OTf})_2(\text{tepo})_3]^+$, 48.47%).

4.8.13. FAB(+)MS spectrum of triethylphosphine oxide-coordinated rare earth (III) chloride. Sc complex. m/z 383 (100%), 385 (63%), 387 (11%), 517 (51%), 519 (33%), 521 (6%).

Y complex. m/z 427 (100%), 429 (83%), 431 (14%), 561 (37%), 563 (24%), 565 (4%).

La complex. m/z 477 (100%), 479 (63%), 481 (11%), 611 (73%), 613 (48%), 615 (9%).

Ce complex. m/z 478 (100%), 480 (74%), 482 (5%), 612 (53%), 614 (41%), 616 (10%).

Pr complex. m/z 479 (100%), 481 (63%), 483 (11%), 613 (31%), 615 (20%), 617 (4%).

Nd complex. m/z 480 (67%), 481 (39%), 482 (100%), 483 (50%), 484 (85%), 485 (26%), 486 (46%), 487 (8%), 488 (26%), 614 (19%), 615 (13%), 616 (29%), 617 (17%), 618 (26%), 619 (10%), 620 (14%), 621 (4%), 622 (8%).

Sm complex. m/z 485 (42%), 486 (37%), 487 (63%), 488 (50%), 489 (33%), 490 (89%), 491 (17%), 492 (100%), 493 (15%), 494 (43%), 495 (7%), 496 (9%), 619 (38%), 620 (36%), 621 (61%), 622 (47%), 623 (36%), 624 (79%), 625 (23%), 626 (92%), 627 (20%), 628 (40%), 629 (9%), 630 (7%).

Eu complex. m/z 489 (64%), 491 (100%), 493 (46%), 495 (7%), 623 (23%), 625 (37%), 627 (18%), 629 (3%).

Gd complex. m/z 492 (11%), 493 (39%), 494 (62%), 495 (67%), 496 (100%), 497 (40%), 498 (95%), 499 (17%), 500 (38%), 502 (6%), 626 (6%), 627 (26%), 628 (41%), 629 (49%), 630 (69%), 631 (33%), 632 (66%), 633 (17%), 634 (27%), 636 (4%).

Tb complex. m/z 497 (100%), 499 (63%), 501 (11%), 631 (53%), 633 (35%), 635 (6%).

Dy complex. m/z 498 (11%), 499 (44%), 500 (66%), 501 (83%), 502 (100%), 503 (48%), 504 (46%), 505 (11%), 506 (7%), 632 (4%), 633 (20%), 634 (30%), 635 (4 1%), 636 (49%), 637 (26%), 638 (23%), 639 (7%), 640 (4%).

Ho complex. m/z 503 (100%), 505 (62%), 507 (11%), 637 (76%), 639 (50%), 641 (10%).

Er complex. m/z 503 (6%), 504 (7 1%), 505 (54%), 506 (100%), 507 (40%), 508 (7 1%), 509 (14%), 510 (24%), 511 (3%), 513 (2%), 637 (3%), 638 (39%), 639 (35%), 640 (59%), 641 (29%), 642 (43%), 643 (11%), 644 (15%), 645 (3%).

Tm complex. m/z 507 (100%), 509 (63%), 511 (11%), 641 (30%), 643 (20%), 645 (3%).

Yb complex. m/z 508 (12%), 509 (33%), 510 (58%), 511 (58%), 512 (100%), 513 (36%), 514 (73%), 515 (13%), 516 (23%), 518 (4%), 642 (5%), 643 (19%), 644 (32%), 645 (36%), 646 (58%), 647 (26%), 648 (43%), 649 (11%), 650 (14%), 652 (2%).

Lu complex. m/z 513 (100%), 515 (63%), 517 (11%), 647 (62%), 649 (41%), 651 (8%).

4.8.14. MS/MS spectra of $[MCl_2(tepo)_3]^+$. $[ScCl_2(tepo)_3]^+$. Precursor ion. m/z 517. Product ions: m/z 249 ($[ScCl_2(tepo)]^+$, 6.20%), 383 ($[ScCl_2(tepo)_2]^+$, 66.59%).

$[YCl_2(tepo)_3]^+$. Precursor ion: m/z 561. Product ions: m/z 293 ($[YCl_2(tepo)]^+$, 9.97%), 427 ($[YCl_2(tepo)_2]^+$, 65.00%).

$[LaCl_2(tepo)_3]^+$. Precursor ion: m/z 611. Product ions: m/z 343 ($[LaCl_2(tepo)]^+$, 18.08%), 477 ($[LaCl_2(tepo)_2]^+$, 71.11%).

$[CeCl_2(tepo)_3]^+$. Precursor ion: m/z 612. Product ions: m/z 344 ($[CeCl_2(tepo)]^+$, 14.68%), 478 ($[CeCl_2(tepo)_2]^+$, 58.01%).

$[PrCl_2(tepo)_3]^+$. Precursor ion: m/z 613. Product ions: m/z 345 ($[PrCl_2(tepo)]^+$, 16.35%), 478 ($[PrCl_2(tepo)_2]^+$, 67.45%).

$[NdCl_2(tepo)_3]^+$. Precursor ion: m/z 616. Product ions: m/z 348 ($[NdCl_2(tepo)]^+$, 16.27%), 482 ($[NdCl_2(tepo)_2]^+$, 72.47%).

$[SmCl_2(tepo)_3]^+$. Precursor ion: m/z 626. Product ions: m/z 358 ($[SmCl_2(tepo)]^+$, 11.06%), 492 ($[SmCl_2(tepo)_2]^+$, 59.49%).

$[EuCl_2(tepo)_3]^+$. Precursor ion: m/z 625. Product ions: m/z 320 ($[Eu^{35}Cl(tepo)]^+$, 5.20%), 322 ($[Eu^{37}Cl(tepo)]^+$, 19.96%), 357 ($[EuCl_2(tepo)]^+$, 4.93%), 454 ($[Eu^{35}Cl(tepo)_2]^+$, 2.07%), 456 ($[Eu^{37}Cl_2(tepo)_2]^+$, 8.72%), 491 ($[EuCl_2(tepo)_2]^+$, 77.54%).

$[GdCl_2(tepo)_3]^+$. Precursor ion: m/z 630. Product ions: m/z 362 ($[GdCl_2(tepo)]^+$, 8.3 1%), 496 ($[GdCl_2(tepo)_2]^+$, 46.44%).

$[TbCl_2(tepo)_3]^+$. Precursor ion: m/z 631. Product ions: m/z 363 ($[TbCl_2(tepo)]^+$, 11.03%), 497 ($[TbCl_2(tepo)_2]^+$, 64.72%).

$[DyCl_2(tepo)_3]^+$. Precursor ion: m/z 636. Product ions: m/z 368 ($[DyCl_2(tepo)]^+$, 12.63%), 502 ($[DyCl_2(tepo)_2]^+$, 76.73%).

$[HoCl_2(tepo)_3]^+$. Precursor ion: m/z 637. Product ions: m/z 369 ($[HoCl_2(tepo)]^+$, 9.33%), 503 ($[HoCl_2(tepo)_2]^+$, 59.05%).

$[ErCl_2(tepo)_3]^+$. Precursor ion: m/z 640. Product ions: m/z 372 ($[ErCl_2(tepo)]^+$, 11.42%), 506 ($[ErCl_2(tepo)_2]^+$, 74.11%).

$[TmCl_2(tepo)_3]^+$. Precursor ion: m/z 641. Product ions: m/z 373 ($[TmCl_2(tepo)]^+$, 10.33%), 507 ($[TmCl_2(tepo)_2]^+$, 70.22%).

$[YbCl_2(tepo)_3]^+$. Precursor ion: m/z 646. Product ions: m/z 378 ($[YbCl_2(tepo)]^+$, 9.05%), 512 ($[YbCl_2(tepo)_2]^+$, 73.41%).

$[LuCl_2(tepo)_3]^+$. Precursor ion: m/z 641. Product ions: m/z 379 ($[LuCl_2(tepo)]^+$, 11.67%), 513 ($[LuCl_2(tepo)_2]^+$, 83.92%).

Acknowledgements

This work was supported by a Grant-in-Aid for Scientific Research from the Ministry of Education, Culture, Sports, Science and Technology, Japan.

References

- For representative reviews, see the following: (a) Kagan, H. B. *Tetrahedron* **1986**, *42*, 6573. (b) Hou, Z.; Wakatsuki, Y.

- Science of Synthesis*; Imamoto, T., Ed.; Thieme: Stuttgart, 2003; Vol. 2, pp 849–942. (c) Kobayashi, S.; Sugiura, M.; Kitagawa, H.; Lam, W. W.-L. *Chem. Rev.* **2002**, *102*, 2227. (d) Shibasaki, M.; Yoshikawa, N. *Chem. Rev.* **2002**, *102*, 2187. (e) Kobayashi, S. *Lanthanides: Chemistry and Use in Organic Synthesis*; Springer: Berlin, 1999. (f) Imamoto, T. *Lanthanides in Organic Synthesis*; Academic: London, 1994. (g) Molander, G. A. *Comprehensive Organic Synthesis*; Trost, B. M., Ed.; Pergamon: Oxford, 1991; Vol. 1.1.9. (h) Imamoto, T. *Comprehensive Organic Synthesis*; Trost, B. M., Ed.; Pergamon: Oxford, 1991; Vol. 1.1.8. (i) Liu, H.-J.; Shia, K.-S.; Shang, X.; Zhu, B.-Y. *Tetrahedron* **1999**, *55*, 3803–3830.
2. For representative reviews and accounts, see: (a) In *Tandem Mass Spectrometry*; McLafferty, F. W., Ed.; Wiley: New York, 1983. (b) In *Mass Spectrometry: Principle and Application*; Hoffmann, E. D., Charette, J., Stroobant, V., Eds.; Wiley: New York, 1996. (c) In *Mass Spectrometry: Principle and Application*; 2nd ed. Hoffmann, E. D., Stroobant, V., Eds.; Wiley: New York, 2001. (d) Biemann, K.; Scoble, H. A. *Science* **1987**, *237*, 992–998. (e) Bush, K. L.; Glish, G. L.; McLuckey, S. A. *Mass Spectrometry/Mass Spectrometry: Techniques and Applications of Tandem Mass Spectrometry*; VCH: New York, 1998.
 3. (a) McLafferty, F. W.; Turecek, F. *Interpretation of Mass Spectra*; University Science Books: Sausalito, 1993. (b) Roepstorff, P. *Curr. Opin. Biotechnol.* **1997**, *8*, 6–13.
 4. Ardrey, B. *Liquid Chromatography/Mass Spectrometry*; VCH: New York, 1993.
 5. (a) Cooks, R. G.; Patrick, J. S.; Kotiaho, T.; McLuckey, S. A. *Mass Spectrom. Rev.* **1994**, *13*, 287–339. (b) Cooks, R. G.; Wong, P. S. H. *Acc. Chem. Res.* **1998**, *31*, 379–386. (c) Cooks, R. G.; Koskinen, J. T.; Thomas, P. D. *J. Mass Spectrom.* **1999**, *34*, 85–92, and references cited therein.
 6. (a) Zhang, D.; Tao, W. A.; Cooks, R. G. *Int. J. Mass Spectrom.* **2001**, *204*, 159–169. (b) Augusti, D. V.; Carazza, F.; Augusti, R.; Tao, W. A.; Cooks, R. G. *Anal. Chem.* **2002**, *74*, 3458–3462. (c) Lianming, W.; Tao, W. A.; Cooks, R. G. *Anal. Bioanal. Chem.* **2002**, *373*, 618–627.
 7. Imamoto, T.; Nishiura, M.; Yamanoi, Y.; Tsuruta, H.; Yamaguchi, K. *Chem. Lett.* **1996**, 875–876.
 8. Part of this work has been reported as a communication Tsuruta, H.; Yamaguchi, K.; Imamoto, T. *Chem. Commun.* **1999**, 1703–1704.
 9. The same erbium complex was also subjected to FAB(–) MS measurement to obtain negative fragmentation patterns. The spectrum indicates four major peaks at *m/z*=1480, 1122, 943, and 764, which were assigned as $[Er(OTf)_4(hmpa)]^-$, $[Er(OTf)_4(hmpa)_2]^-$, $[Er(OTf)_4(hmpa)]^-$, and $[Er(OTf)_4]^-$. A peak corresponding to $[Er(OTf)_4(hmpa)_3]^-$, was not clearly observed in this negative MS, probably because this ion was very unstable to readily release the HMPA molecule.
 10. Yanagihara, N.; Nakamura, S.; Nakayama, M. *Chem. Lett.* **1995**, 555–556.
 11. When the metal element of the complex contains multi isotopes, we selected the precursor ion that consists of the isotope with the greatest natural abundance. Of course, however, the same results were obtained when an isotope of a lower natural abundance was selected.
 12. (a) Martin, W. C.; Hangan, L.; Reader, J.; Sugar, J. *J. Phys. Chem. Ref. Data* **1974**, *3*, 771. (b) Morss, L. R. *Chem. Rev.* **1976**, *76*, 827–842.
 13. The transformation of $[M(OTf)_2(hmpa)_2]^+$ to $[MF(OTf)(hmpa)_2]^+$ involves both the M–OTf bond fission and the M–F bond formation. We assume that these two processes occur simultaneously via a cyclic transition state.
 14. (a) Sinha, S. P. In *Systematics and the Properties of the Lanthanides*; Sinha, S. P., Ed.; Reidel: Dordrecht, 1983; p 71. (b) Sinha, S. P. *Helv. Chim. Acta* **1978**, *1975*, 58. (c) Sinha, S. P. *Struct. Bonding* **1976**, *30*, 1.
 15. (a) Peppard, D. F.; Mason, G. W.; Lewey, S. *J. Inorg. Nucl. Chem.* **1960**, *31*, 2271. (b) Peppard, D. F.; Bloomquist, C. A. A.; Horwitz, E. P.; Lewey, S.; Mason, G. W. *J. Inorg. Nucl. Chem.* **1970**, *32*, 519. (c) Siekierski, S. *J. Inorg. Nucl. Chem.* **1970**, *32*, 519.
 16. Nugent, L. J. *J. Inorg. Nucl. Chem.* **1970**, *32*, 3485.
 17. These facts are consistent with the data obtained from X-ray crystallographic analysis of a series of HMPA-coordinated lanthanide triflates. The Sc and Yb complexes show relatively long P–O bond lengths of the coordinated HMPA molecules. It is reasonable to consider that the P–O bond elongations are due to the relatively strong Lewis acidity of Sc(III) and Yb(III).
 18. Ytterbium(III) salts generally exhibit higher catalytic activity than lutetium(III) salts although the ionic radius of Yb^{3+} is larger than that of Lu^{3+} . (a) Takaki, K.; Nagase, K.; Beppu, F.; Fujiwara, Y. *Chem. Lett.* **1991**, 1665–1668. (b) Kawada, A.; Mitamura, S.; Kobayashi, S. *J. Chem. Soc., Chem. Commun.* **1993**, 1157–1158. (c) Kobayashi, S.; Ishitani, H. *J. Am. Chem. Soc.* **1994**, *116*, 4083–4084. (d) Kobayashi, S.; Ishitani, H. *J. Org. Chem.* **1994**, *59*, 3590–3596. (e) Kobayashi, S.; Ishitani, H.; Nagayama, S. *Synlett* **1995**, 1195–1202. (f) Hanamoto, T.; Sugimoto, Y.; Jin, Y. Z.; Inanaga, J. *Bull. Chem. Soc. Jpn.* **1997**, *70*, 1421–1426. (g) Yamanaka, M.; Nishida, A.; Nakagawa, M. *J. Org. Chem.* **2003**, *3112*, 3120.
 19. Asakura, K.; Yamaguchi, K.; Imamoto, T. *Chem. Lett.* **2000**, 424–425.
 20. Nishiura, M.; Okano, N.; Imamoto, T. *Bull. Chem. Soc. Jpn.* **1999**, *72*, 1793–1801.
 21. We examined other combinations of two kinds of product ion and found that the quotients $\ln\{[MF_2(\text{ligand})_2]^+ / [MF(OTf)(\text{ligand})]^+\}$ (ligand=hmpa, tepo, tmp, and dmso) are directly proportional to the atomic number of the lanthanides and they also correlate well with the ionic radius except scandium. Representative examples are shown in Figures 18 and 19. These results have not yet been well rationalized, but we assumed that the quotients indicate the relative strength of the fluorophilicity of the rare earth elements.

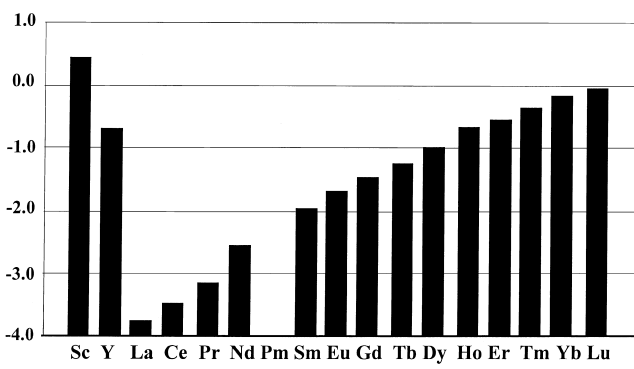


Figure 18. MS/MS ion peak ratio, $\ln\{[MF_2(hmpa)_2]^+ / [MF(OTf)(hmpa)]^+\}$.